J KAU: Earth Sci., **vol. 5**, pp. 49-79 (1412 A.H./1992 A.D.)

Petrology and Copper Geochemistry of the Lower Part of the Tertiary Yemen Volcanics, Utma Area, Yemen Republic

SALAH AL-KHIRBASH and TAREQ H. AL-HIBSHI
Geology Department, Faculty of Science,
Sana'a University, Sana'a, Yemen Republic.

ABSTRACT. This study concludes that the rocks from the lower sequence of the Tertiary Yemen Volcanics, in the Utma area are composed of porphyritic, intergranular, and uncommonly spinifex textured clinopyroxene (augite and diopside), olivine, ca-plagioclase, and magnetite. This sequence is interpreted to represent mafic, non-cumulate effusive volcanite that formed at shallow depth. Pumpellyite, chlorite, glass, magnetite, sphene, epidote, serpentine, and calcite are among the secondary minerals that were formed by subsequent low-grade metamorphism.

Geochemical analyses and norm calculations of 33 representative samples from the Utma lower sequence suggest that the rocks are undersaturated, high-Mg tholeiites characterized by high MgO, TiO_2, Ni, and Cr and by low SiO_2, Al_2O_3, and alkalies contents. Silica, MgO, Sr, Cu, and possibly Ni were remobilized during alteration and low-grade metamorphism, while TiO_2, Cr, Nb, Zr were immobile and very much controlled by fractional crystallization.

Geochemical data from Utma were compared with data from various parts of the world and plotted in CaO-MgO-Al_2O_3 and Al_2O_3 vs. FM diagrams. This study shows that the analyzed rocks resemble those of the Barberton low Al-rock series (Viljoen and Viljoen 1969), with high TiO_2 and F/(F+M) values and possibly they are not komatiites.

Ore microscopy shows the presence of very fine-grained disseminated, veinlets, and amygdale-filled with native copper. Copper is abundant along fractures and joint surfaces. Analysis for Cu of separated silicate and iron-oxide fractions shows that the silicate minerals are the source of syngenetic copper, copper was leached and reconcentrated epigenetically in amygdales and fractures, along with hematite. Pumpellyitization of primary minerals produced metamorphic fluids with favorable geochemical conditions for the precipitation of native copper.

Introduction

Widespread volcanic activity occurred in the Yemen and adjacent areas during the Late Cretaceous and Early Tertiary which is believed to be associated with the vertical uplift of the Afro-Arabian dome and rifting of the Red Sea (Gass 1970; Chiesa *et al.* 1983; Almond 1986; Camp and Roobol 1989). As a result tremendous amounts of fissure-erupted and caldera eruptive centers, dykes and volcanic flows were formed, particularly in the central highlands of the country, covering almost 45,000 sq. km (Heyckendorf and Jung 1989) (Fig. 1).

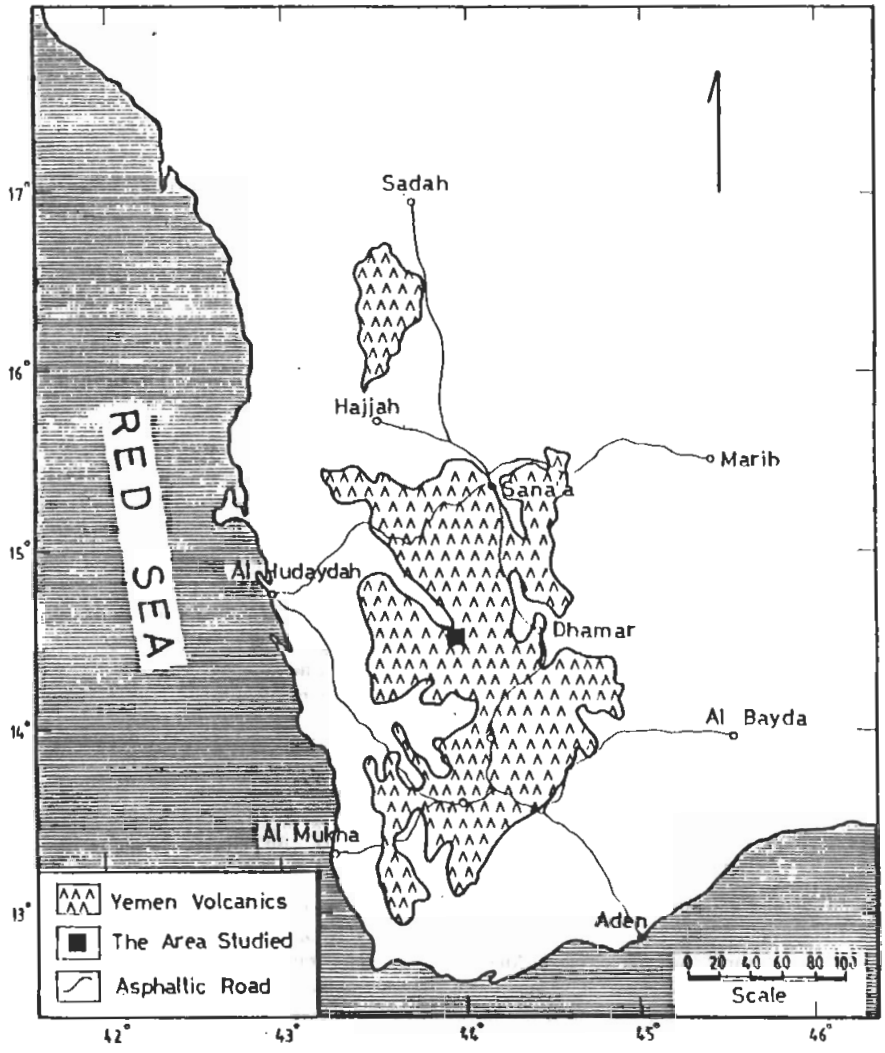

FIG. 1. Location map of the study area and extent of the Tertiary Yemen Volcanics.

Previous research on the geology and geochemistry of these volcanic rocks can be summarized as follows: Guekens (1966) studied their general distribution within the general stratigraphic column of Yemen and called them "Trap Series". Grolier and Overstreet (1978) and Kruck (1983) renamed them the "Yemen Volcanics" and "basaltic plateau of Yemen", as defined by Capaldi *et al.* (1987a). Grolier and Overstreet (1978) have looked more closely at the petrology and chemistry in some selected areas. The Yemen Volcanics are composed mainly of basalts, andesites, trachyandesites, trachytes, rhyolites, ignimbrites, and tuffs. There are also subordinate fresh-water "Inter-Trap" sediments that represent quiescent periods during the Cretaceous-Early Tertiary volcanic activity. The above studies showed a gradual change of rock composition from the bottom (basic rocks) to the top (acidic rocks) of the section.

The precise age of the Yemen volcanics age is not well established, K/Ar dating by Civetta *et al.* (1978) gave a 30-21 Ma for the extrusive rocks around the Dhamar-Rada volcanic field. Whereas, Menzies *et al.* (1990) reported an age of 43.5 ± 21.2 Ma for the eruption of the basal alkaline volcanics. Civetta *et al.* (1978) concluded that there were at least two distinct periods of volcanic activity. In the north-central part of Yemen, volcanic activity ended in the Upper Oligocene (26 Ma) and was represented by a thick sequence of differentiated basaltic rocks, rhyolites, and peralkaline ignimbrites, while it continued in the southern parts of the country at least until the Lower Miocene (19 Ma) producing a wide range of volcanic assemblages (Capaldi *et al.* 1987a). The youngest volcanic rocks range between 10 and 5 Ma (Capaldi *et al.* 1987b, c; Huchon *et al.* 1990).

Earlier studies on the Tertiary Yemen volcanics concluded there was absence of any mineralization (e.g. Grolier and Overstreet 1978; Overstreet *et al.* 1985), and also the absence of rocks that are more basic than basalts (e.g. Heyckendorf and Jung 1989). The presence of disseminated native copper in the lower sections of the Utma rocks, which has been observed for the first time by the first author, and the peculiar appearance of these rocks attracted studies in order to determine the nature and petrogenesis of these rocks and to study the distribution and behavior of the copper mineralization and other elements during alteration and low-grade metamorphism.

The area under investigation is located about 45 km west of Dhamar city (Fig. 1). It is entirely underlain by the Tertiary volcanic rocks which are cut by several dykes and crossed by wadies and major faults striking NW-SE. The volcanic rocks comprise a wide range of rock compositions, from basic rocks in the lower sections of the lava pile where they are locally subjected to low-grade metamorphism, to trachy-andesite, trachyte, and rhyolite at higher horizons.

Metamorphic Petrography of the Utma Lavas

Examination of several thin sections reveals that alteration and low-grade metamorphism have destroyed some of the original mineralogy of the rocks. However, alteration does not produce penetrative deformation, so that original textures

are abundant and visible. The use of such textures and the relics of primary minerals, allow the determination of the original mineralogy in most thin sections. Extensive readjustment took place primarily in amygdaloidal zones, breccias, or along fractures. Porphyritic, cluster, and intergranular textures are dominant; spinifex textures have been preserved in some samples, in which large crystals of clinopyroxene lie in a matrix of smaller prismatic clinopyroxene crystals and devitrified glass (Fig. 2). Generally, these textures are believed to be related to the cooling history of the lavas, where as in this case they are suggestive of rapid cooling (see for example Augustithis 1978).

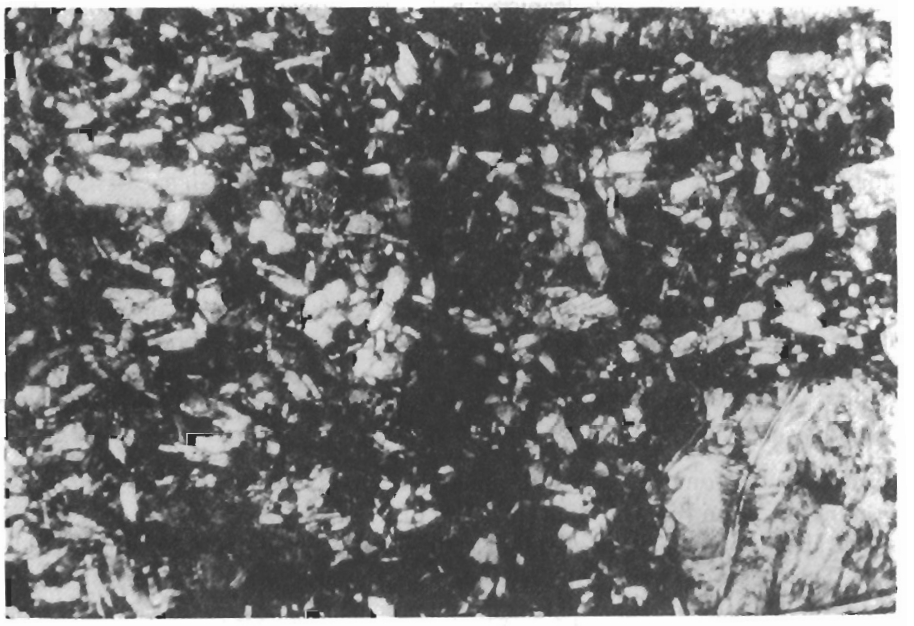

FIG. 2. Photomicrograph showing clinopyroxene crystals in a matrix of clinopyroxene and devetrified glass, sample # 13, (×4).

Pseudomorphs of relict, skeletal and rarely zoned clinopyroxene (34%, titanoaugite and diopside) and skeletal, equant phenocrysts of olivine (10%) are the most common minerals (Fig. 3). They have been altered to chlorite (12%), iron oxides (8%), and such accessories as epidote, serpentine, actinolite-tremolite (10%) and calcite (4%). Basaltic hornblende after clinopyroxene is present in some thin sections interstitial. Orthopyroxene (commonly hypersthene) and biotite are also present (samples no. 10 and 14A) and were recognized by their schiller structure and parallel extinction, respectively. Hypersthene is surrounded by a reaction rim of augite and is commonly altered to chlorite. Inclusions of prismatic apatite and sphene are present as alteration products. Sphene, along with iron-oxides (magnetite), is concentrated along the pyroxene and olivine phenocryst edges (possibly as a resut of serpentinization), where the former is characterized by its rhomb shape. Zircon is present as small grains within the pyroxene crystals (Fig. 4).

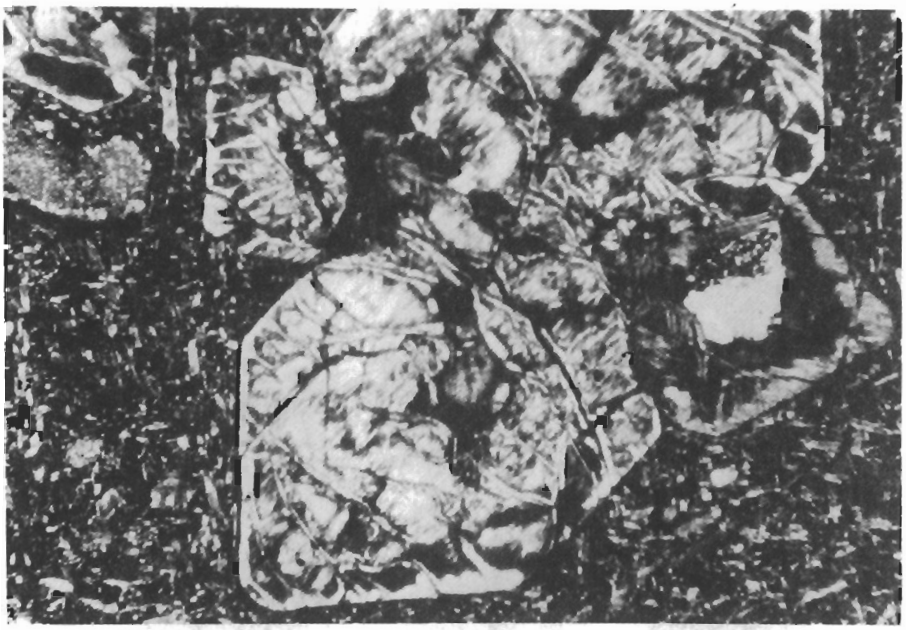

FIG. 3. Photomicrograph showing pseudomorphs of relict and skeletal clinopyroxene and olivine crystals, sample # 19, (×4).

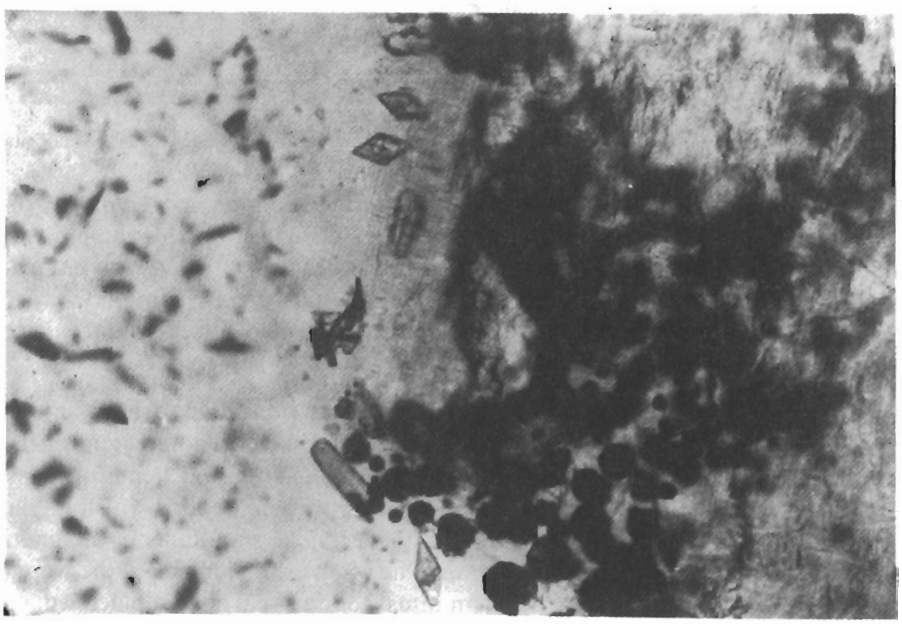

FIG. 4. Small crystals of sphene, zircon, and apatite, concentrated along the edges of the phenocryst, sample # 2, (×40).

Amygdales, on the other hand represent an important part of the rock composition, as they acted as channelways for the metamorphic fluids. They are commonly rimmed with chlorite and iron oxides, and cored with quartz, fan-shaped chalcedony, calcite, clinozoisite, prehnite(?)-pumpellyite, native copper, and other opaque minerals (Fig. 5). The prehnite-pumpellyite occur in the typical form as radiating masses of faintly greenish color.

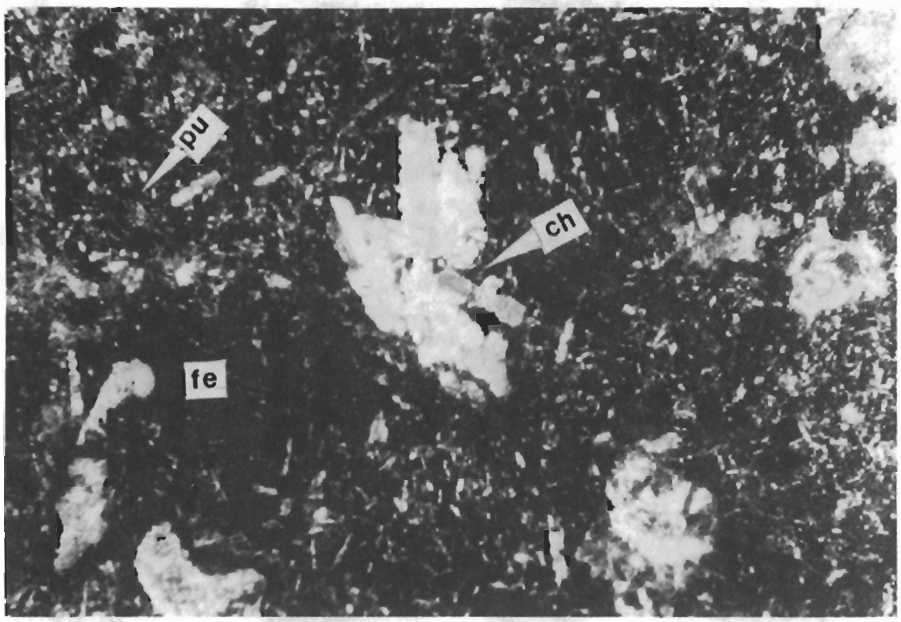

FIG. 5. Photomicrograph showing chlorite (ch), pumpellyite (pu), and iron-oxide (fe) as the main alteration of low-grade metamorphism, sample # 19, (×4).

The groundmass represents about 54% of the rock and is composed mostly of altered low calcium pyroxenes (pigeonite or subcalcic augite), opaque minerals, clay minerals (after plagioclase), and dark-brown glass that devitrified into chloritoid minerals (pumpellyite). Unaltered plagioclase crystals are present; however, in some thin sections it was so difficult to distinguish between plagioclase and pyroxene crystals mainly due to their intense alteration.

Epidote, calcite, serpentine (antigorite), and talc are present in variable amounts. Epidote might be formed by late stage (deuteric) chemical readjustment of mafic minerals. Iron oxides are mainly in the form of magnetite and hematite phases. Euhedral and subhedral crystals of magnetite are embedded in the glassy groundmass as a symplectic intergrowth suggesting a simultaneous magnetite-groundmass crystallization. Exsolution lamellae of ulvospinel in magnetite were observed in some thin sections (Fig. 6). Hematite is found as partially replacing magnetite grains, coating fractures, and grain boundaries in some places associated with native copper.

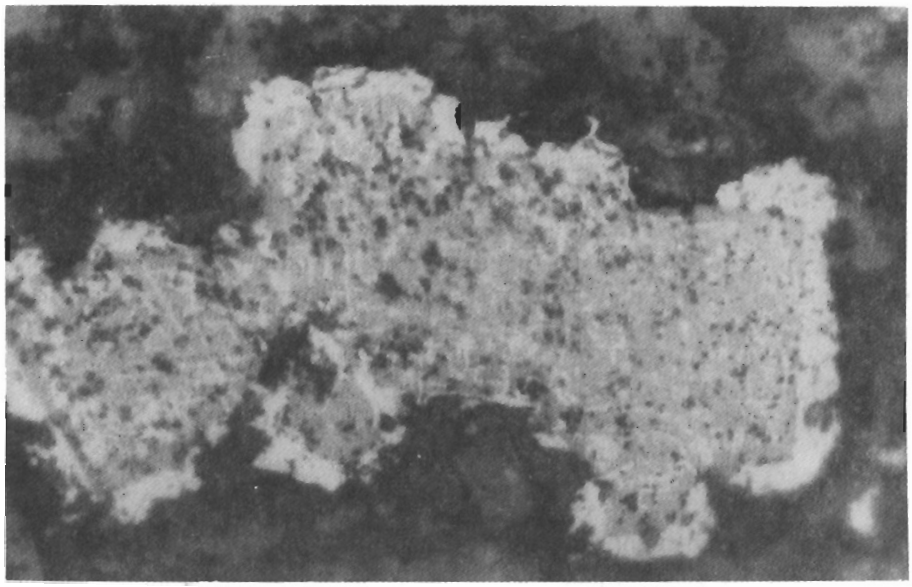

FIG. 6. Exsolution of ulvospinel from magnetite, sample # 12, (×50).

Corona and cluster structures, and phenocrysts with magmatic corroded edges have been observed in some thin sections (Fig. 7) and they have developed as a result

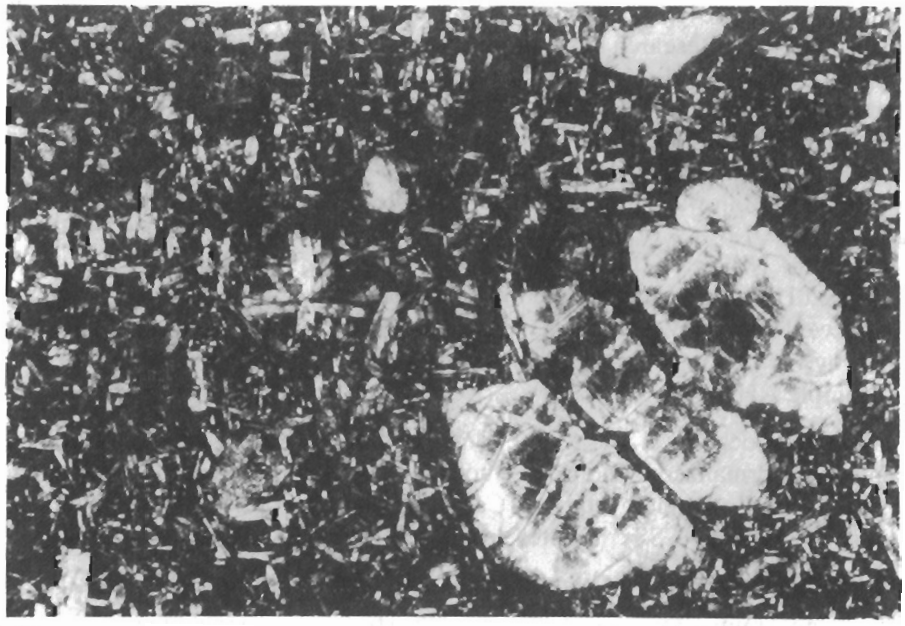

FIG. 7. Photomicrograph showing corona and cluster structures and corroded crystal edges, sample # 14A, (×10).

of late magmatic interaction of phenocrysts with the basaltic melt (Augustithis 1978).

X-ray diffraction analyses of seven samples were carried out at the USGS-Jeddah laboratory. The results indicate the presence of augite, diopside, magnetite, talc, serpentine (lizardite), hematite, trace amounts of clinochlore and zeolites (natalite) and other low temperature alteration products of silicate minerals.

The presence of calcite-filled veins, tremolite-actinolite minerals (associated with some of the pyroxenes) and amphibole pseudomorphs after clinopyroxene indicate low-temperature hydrothermal activity, possibly post-dating the volcanic eruption. Broken phenocrysts, bent plagioclase twins, and cracks filled with calcite and groundmass material are evidence that crystal fracturing and brittle deformation were caused by gas explosion during volcanism, sudden temperature changes, and possibly magmatic collision of the phenocryst during lava motion.

Geochemistry of Lower Sequence of Utma Rocks

Analytical Techniques

Major and selected minor elements were performed on 35 representative samples (Table 1). Twenty-nine samples, referred to in the text as Group 1 were collected from the lower part of the Utma Tertiary volcanic sequence. Four samples (numbered A1, B1, B2, D and referred to as Group 2) are unaltered and were collected from few meters above the first group. Two samples (designated AH and BM) from the basal basalts of the Tertiary volcanics from different areas are included for comparison. The samples were analyzed by the authors using the Rb-target Rigako XRF unit at the Central Research Laboratory, Faculty of Science, Sana'a University. Five grams of crushed sample (100-200 μm) were mixed with one gram of boric acid powder and pressed to pellets. Eight U.S.G. Survey rock standards (BHVO-1, MAG-1, QLO-1, RGM-1, SCO-1, SDC-1, SGR-1, and STM-1) were used as standards (Gladney and Goode 1981). Precision of the analyses was determined from standard curve deviations, as follows: $SiO_2 \pm 3.7\%$; Al_2O_3, Fe_2O_3, $FeO \pm 0.5\%$; $TiO_2 \pm 0.26\%$; MgO, $CaO \pm 1.8\%$; MnO, Na_2O, K_2O, $P_2O_5 \pm 0.03\%$; $H_2O \pm 3.4\%$; Cu, Zn ± 20ppm; Ni, Sr ± 64ppm; Nb, Zr, Co ± 5ppm; Cr ± 224ppm. Water content (H_2O^+ and H_2O^-) were determined following the precedure described by Johnson and Maxwell (1981). Wet chemistry was applied for the determination of FeO as described by Hutchison (1974). The values were adjusted using Fe_2O_3 / FeO ratio of 0.44 (sample AH).

Obtained geochemical data were processed to give the various petrological parameters, normalized oxide values, normative minerals, and petrologic diagrams using the IGPET computer program (Carr 1985); and the statistical parameters were processed using the NCSS computer program (Hintze 1986).

Chemical Characteristics of Utma Rocks

The original mineralogy and chemistry of the studied Utma rocks has been complicated by subsequent alteration and low-grade metamorphism. In thin section the

TABLE 1. Analyses of major oxides (wt %), minor elements (ppm), and CIPW norms of Utma rocks (recalculated 100% anhydrous) and analyses of rocks from different regions.

Sample #	1	2	2A	3	6	6A	6B	7A	7B	8	8A	9	10	10A	11	12	13	14a
Group #	1	1	1	1	1	1	1	1	1	1	1	1	1	1	1	1	1	1
SiO_2	38.40	40.41	40.47	40.90	38.50	38.55	37.17	40.97	40.65	41.94	41.87	38.41	42.51	37.74	41.79	40.83	41.63	40.58
TiO_2	2.32	2.82	2.82	2.35	2.62	2.60	2.88	2.56	2.52	2.33	2.32	3.57	2.29	2.43	2.23	2.38	2.26	2.42
Al_2O_3	4.39	5.45	5.51	4.85	5.05	5.04	4.77	4.54	4.68	4.38	4.29	6.43	4.01	4.48	4.17	4.53	4.33	4.84
Fe_2O_3	6.75	5.58	5.46	5.24	7.04	6.99	7.72	6.13	5.82	5.75	5.99	5.73	6.00	6.16	6.36	5.95	6.64	6.77
FeO	7.81	7.17	7.05	6.76	8.59	8.52	9.44	7.80	7.40	7.22	7.97	6.67	7.71	7.20	7.36	7.43	7.75	7.99
MnO	0.21	0.27	0.27	0.29	0.23	0.22	0.25	0.24	0.29	0.25	0.25	0.19	0.25	0.24	0.16	0.21	0.21	0.22
MgO	29.16	24.50	24.67	27.36	26.67	26.55	25.42	23.11	24.31	25.40	24.73	24.95	22.01	25.60	27.77	27.11	27.22	26.73
CaO	10.43	13.18	13.10	11.70	10.79	10.97	11.70	14.03	13.79	12.26	12.09	13.38	14.67	15.59	9.78	10.96	9.41	10.03
Na_2O	0.03	0.02	0.12	0.12	0.13	0.13	0.14	0.12	0.13	0.12	0.11	0.11	0.13	0.13	0.11	0.11	0.11	0.11
K_2O	0.08	0.09	0.09	0.09	0.06	0.09	0.12	0.08	0.08	0.07	0.07	0.07	0.07	0.09	0.04	0.11	0.10	0.05
P_2O_5	0.30	0.43	0.43	0.32	0.32	0.31	0.35	0.36	0.38	0.34	0.35	0.46	0.34	0.36	0.30	0.35	0.27	0.28
Total	**99.9**	**99.9**	**100.0**	**100.0**	**100.0**	**99.97**	**99.96**	**100.0**	**100.05**	**100.06**	**100.04**	**99.9**	**100.0**	**100.02**	**99.9**	**99.9**	**99.93**	**100.02**
Cu	29	104	65	34	75	82	68	39	24	22	29	22	56	69	75	78	53	45
Ni	473	488	479	476	465	467	438	475	466	463	469	122	460	458	465	428	479	455
Sr	309	431	433	387	338	341	319	420	413	414	416	254	273	279	206	306	312	324
Nb	25	29	30	25	25	25	27	24	25	23	24	38	25	25	26	27	25	25
Zr	115	142	144	124	130	125	123	130	129	131	131	143	114	116	110	132	117	123
Cr	1703	1481	1444	1859	1493	1556	1342	1444	1525	1711	1627	796	1237	1316	1520	1687	1579	1813
Zn	83	83	80	84	114	98	79	76	98	133	79	101	156	112	70	75	71	75
Co	86	70	76	74	76	78	75	70	74	73	73	53	65	66	79	76	78	76
AN	100	100	100	100	100	100	100	100	100	98.2	92.1	100	100	100	92.1	100	92.0	93.1
Or	0.0	0.0	0.0	0.0	0.0	0.0	0.0	0.0	0.0	0.4	0.4	0.0	0.0	0.0	0.2	0.0	0.6	0.3
ab	0.0	0.0	0.0	0.0	0.0	0.0	0.0	0.0	0.0	0.2	0.9	0.0	0.0	0.0	0.9	0.0	0.9	0.9
an	10.9	12.7	12.8	11.6	11.4	11.3	9.3	10.3	10.8	10.7	10.6	16.3	8.7	9.8	10.8	11.5	10.6	12.0
lc	0.4	0.4	0.4	0.4	0.2	0.4	0.4	0.3	0.3	0.0	0.0	0.3	0.3	0.4	0.0	0.5	0.0	0.0
ne	0.1	0.1	0.5	0.5	0.5	0.5	0.5	0.5	0.5	0.4	0.0	0.5	0.5	0.5	0.0	0.5	0.0	0.0
di	15.2	28.3	28.7	27.7	17.8	17.9	13.1	32.1	29.6	35.8	35.7	22.2	38.8	13.4	28.4	30.8	25.8	26.8
hy	0.0	0.0	0.0	0.0	0.0	0.0	0.0	0.0	0.0	0.0	0.6	0.0	0.0	0.0	4.8	0.0	5.7	0.4
ol	51.9	32.9	33.8	40.8	43.4	42.8	38.1	31.7	34.7	37.5	37.3	37.4	26.9	40.3	44.5	45.0	2.0	44.5
mt	5.4	5.8	5.8	5.3	5.5	5.5	5.4	5.5	5.5	5.4	5.4	7.2	5.0	5.2	5.4	5.6	5.3	5.5
il	4.2	4.7	4.8	4.1	4.4	4.3	4.2	4.3	4.3	4.2	4.3	6.6	3.7	4.0	4.2	4.5	4.1	4.4
ap	0.7	0.9	0.9	0.7	0.7	0.6	0.6	0.7	0.8	0.7	0.8	1.0	0.7	0.7	0.7	0.8	0.6	0.6

TABLE 1. (cont.) Analyses of major oxides (wt %), minor elements (ppm), and CIPW norms of Utma rocks (recalculated 100% anhydrous) and analyses of rocks from different regions.

Sample #	1	2	2A	3	6	6A	6B	7A	7B	8	8A	9	10	10A	11	12	13	14a
Group #	1	1	1	1	1	1	1	1	1	1	1	1	1	1	1	1	1	1
COS	5.2	2.0	2.0	1.6	3.4	3.7	5.4	2.6	3.4	0.0	0.0	5.2	0.9	11.7	0.0	0.5	0.0	0.0
FeO*	13.09	10.71	10.74	10.66	13.06	12.91	12.67	11.75	11.39	11.83	12.91	11.44	11.23	10.96	13.11	12.78	13.1	13.48
F/F+M	0.326	0.33	0.33	0.301	0.36	0.361	0.395	0.370	0.347	0.332	0.348	0.325	0.377	0.336	0.323	0.324	0.339	0.349
den	2.84	2.89	2.89	2.89	2.88	2.88	2.90	2.88	2.88	2.87	2.87	2.83	2.88	2.85	2.80	2.87	2.80	2.82
Sample #	14aa	14B	14C	14Cc	14D	14Dd	15	16	17B	18	20	A1	B1	B2	D	BM	AH	
Group #	1	1	1	1	1	1	1	1	1	1	1	2	2	2	2	3	3	
SiO_2	40.46	40.51	44.67	43.42	40.29	40.70	41.65	45.61	42.71	44.59	43.87	46.15	43.14	43.11	43.22	40.93	45.06	
TiO_2	2.42	2.50	2.23	2.24	2.65	2.68	2.13	2.08	2.38	2.19	2.60	2.55	2.47	2.84	2.18	4.70	2.36	
Al_2O_3	4.86	4.85	4.00	4.16	5.08	4.57	4.15	4.35	4.15	4.27	5.01	6.06	4.46	6.22	4.65	14.10	14.62	
Fe_2O_3	6.50	6.48	5.71	5.64	6.55	6.78	5.77	5.56	6.22	5.84	6.21	5.98	5.87	5.50	6.15	3.96	5.93	
FeO	8.08	8.12	7.20	7.18	8.28	7.85	7.75	7.03	7.20	7.39	7.18	7.00	7.35	7.11	7.60	8.91	7.70	
MnO	0.22	0.22	0.24	0.24	0.26	0.26	0.25	0.24	0.24	0.22	0.26	0.15	0.20	0.23	0.20	0.20	0.34	
MgO	26.80	26.62	24.74	26.05	25.46	25.09	27.45	25.28	26.62	25.60	22.60	20.14	25.71	22.31	25.61	9.31	8.94	
CaO	10.23	10.22	10.74	10.59	10.90	11.06	10.22	9.42	10.02	9.44	11.74	10.00	10.25	12.11	9.75	13.83	10.39	
Na_2O	0.11	0.11	0.12	0.11	0.11	0.11	0.11	0.11	0.11	0.11	0.11	1.02	0.25	0.10	0.26	2.90	3.79	
K_2O	0.05	0.07	0.05	0.05	0.05	0.07	0.05	0.05	0.09	0.09	0.06	0.59	0.05	0.03	0.08	0.50	0.59	
P_2O_5	0.29	0.29	0.30	0.30	0.30	0.30	0.27	0.26	0.28	0.25	0.36	0.32	0.31	0.41	0.27	0.61	0.29	
Total	**100.02**	**99.98**	**100.0**	**99.98**	**99.93**	**99.80**	**100.08**	**99.99**	**100.02**	**99.99**	**100.0**	**99.96**	**100.06**	**99.97**	**99.97**	**99.95**	**100.01**	
Cu	56	49	34	31	57	54	61	62	56	52	37	88	68	59	43	33	67	
Ni	482	480	482	484	456	445	508	507	485	514	493	461	474	279	417	81	72	
Sr	319	329	417	415	316	318	336	414	306	315	424	260	270	253	347	420	265	
Nb	24	23	22	24	27	26	23	24	28	25	28	26	27	32	26	21	11	
Zr	125	124	127	128	132	129	124	129	125	119	147	141	126	152	122	133	133	
Cr	1876	1763	1621	1590	1540	1530	1754	1892	1493	1619	1643	2302	1523	1133	1723	620	381	
Zn	75	76	79	85	85	90	93	91	102	99	77	149	105	89	95	86	51	
Co	78	76	67	74	76	76	72	78	76	76	67	76	76	66	69	56	51	
AN	98.2	94.6	91.4	91.8	100.0	93.1	92.0	92.3	91.6	92.0	93.2	54.2	83.6	95.0	83.7	53.7	40.8	
Or	0.3	0.4	0.3	0.3	0.1	0.3	0.3	0.3	0.5	0.5	0.4	3.4	0.0	0.0	0.0	0.0	0.0	
ab	0.2	0.7	0.9	0.9	0.0	0.9	0.9	1.0	0.9	0.9	0.9	8.5	0.3	0.2	0.5	2.8	2.9	
an	12.2	12.1	9.7	10.3	12.5	11.9	10.4	11.5	10.2	10.8	12.8	10.0	2.1	0.9	2.1	18.1	25.6	
lc	0.0	0.0	0.0	0.0	0.1	0.0	0.0	0.0	0.0	0.0	0.0	0.0	10.8	16.3	10.9	20.9	17.7	

ne	0.4	0.1	0.0	0.0	0.5	0.0	0.0	0.0	0.0	0.0	0.0	0.0	0.0	0.0	0.0	1.8	0.6
di	27.9	27.8	30.9	30.1	29.1	28.7	30.5	27.4	28.6	26.9	33.3	29.0	29.6	32.0	27.0	28.4	19.2
hy	0.0	0.0	17.6	11.3	0.0	0.2	1.5	27.6	9.6	21.3	15.2	15.1	10.7	12.9	11.1	0.0	0.0
ol	45.0	44.4	25.5	32.7	40.7	37.8	43.4	24.6	36.3	28.4	23.9	20.6	34.2	24.2	34.7	8.4	13.0
mt	5.6	5.7	5.3	5.3	5.8	5.7	5.2	5.3	5.5	5.3	5.9	5.8	0.0	0.0	0.0	0.0	0.0
il	4.5	4.6	4.0	4.1	4.8	4.6	3.9	4.1	4.4	4.1	4.8	4.8	5.7	6.3	5.2	5.0	5.0
ap	0.7	0.7	0.7	0.7	0.7	0.7	0.6	0.6	0.6	0.6	0.8	0.7	4.6	5.3	4.0	7.8	3.7
COS	0.0	0.0	0.0	0.0	0.0	0.0	0.0	0.0	0.0	0.0	0.0	0.0	0.7	1.0	0.6	1.2	0.6
FeO*	13.50	13.49	11.73	11.74	13.39	12.71	12.60	12.36	12.41	12.57	12.53	12.16	12.50	11.93	12.65	10.90	10.91
F/F+M	0.345	0.347	0.337	0.324	0.362	0.362	0.314	0.327	0.329	0.335	0.366	0.384	0.333	0.355	0.343	0.577	0.600
den	2.87	2.88	2.83	2.86	2.89	2.80	2.87	2.82	2.79	2.83	2.76	2.72	2.86	2.84	2.85	2.74	2.67

TABLE 1. (cont.) Analyses of major oxides (wt %), minor elements (ppm), and CIPW norms of Utma rocks (recalculated 100% anhydrous) and analyses of rocks from different regions.

Sample #	NP1	NP2	NP3	NP4	NP5	NP6	NP7	NP8	MT1	MT2	MT3	MT4	MT5	MT6	K1	K2	K3
Group #	4	4	4	4	4	4	4	4	5	5	5	5	5	5	6	6	6
SiO_2	42.08	43.72	43.82	43.86	44.50	42.90	42.64	43.20	44.0	44.20	44.4	45.6	43.5	45.9	45.75	47.19	45.95
TiO_2	2.67	1.90	1.86	1.99	1.29	1.16	1.12	1.20	0.15	0.18	0.35	0.27	0.44	0.3	0.73	0.76	1.28
Al_2O_3	9.01	8.59	7.11	6.97	8.16	7.18	6.99	7.47	4.1	5.02	7.4	7.35	9.24	6.66	8.85	8.28	6.34
Fe_2O_3	4.45	4.17	3.07	3.02	5.82	6.77	5.77	6.12	9.0	10.4	13.3	11.7	13.5	11.4	–	–	–
FeO	11.60	11.30	12.48	11.83	7.87	7.99	8.38	8.06	–	–	–	–	–	–	12.97*	12.34*	15.88*
MnO	0.91	0.17	0.18	0.17	0.15	0.15	0.15	0.15	0.16	0.21	0.26	0.21	0.21	0.24	0.19	0.26	0.17
MgO	13.76	13.18	17.40	14.70	18.48	21.21	21.46	20.20	38.6	34.5	27.5	25.9	23.4	28.6	21.34	20.64	19.61
CaO	9.56	9.81	8.93	11.25	7.31	5.23	5.72	6.78	3.61	4.34	6.33	7.62	9.26	6.34	8.62	8.96	9.14
Na_2O	0.40	0.60	0.26	0.30	0.48	0.38	0.30	0.36	0.08	0.30	0.06	0.83	0.12	0.21	0.04	0.21	0.20
K_2O	0.16	0.20	0.15	0.11	0.26	0.15	0.14	0.12	0.11	0.02	0.08	0.06	0.01	0.12	0.00	0.02	0.04
P_2O_5	0.27	–	–	–	0.08	0.07	0.07	0.07	–	–	–	–	–	–	–	–	–
LOI	6.08	6.09	–	4.69	5.69	6.66	6.86	6.37	9.3	6.9	7.4	3.1	6.2	7.8	–	–	–
Total	**100.16**	**99.73**	**–**	**98.89**	**100.04**	**99.85**	**99.54**	**100.10**	**100.3**	**100.1**	**100.8**	**100.1**	**100.9**	**99.9**	**98.49**	**98.66**	**98.61**
Cu	170	210	830	170	140	110	120	180	–	–	–	–	–	–	–	–	–
Ni	600	600	850	840	770	780	840	860	2290	–	1470	–	980	1706	1048	931	1361
Cr	750	740	1222	800	–	–	–	–	1762	–	3080	–	3272	2263	3028	3438	3492
Co	60	60	70	80	80	80	80	80	118	–	122	–	109	118	–	72	122

(–) not determined, (*) Total Fe as FeO.

Key to Groups No. : (1 & 2) = rocks from Utma, (3) = rocks from Tertiary Yemen volcanics, (4) = ultramafic volcanic rocks from Noril'sk and Pechenga Provinces (USSR), (5) = komatiites from Munro Township (Canada), (6) = amphibolites from Kolar Belt (India).

presence of secondary minerals such as pumpellyite, chlorite, iron oxides, tremolite-actinolite, epidote, calcite, sphene, clinozoisite and clay minerals suggests that the original phenocrysts (olivine, clinopyroxene), and plagioclase have been altered during hydrothermal and low-grade metamorphism.

The analyzed samples of the lower section (Group 1) and those of Group 2 are characterized by low average contents of SiO_2 (41.09%), Al_2O_3 (4.66%), Na_2O (0.11%), K_2O (0.06%) and high average contents of MgO (25.64%), CaO (11.47%), Fe_2O_3 (6.65%), whereas their FM value is 0.32-0.37. The high CaO content is apparently due to serpentinization of olivine and uncommonly the presence of secondary calcite-filled veins. The high Fe_2O_3 is attributed to the oxidation of the opaque minerals. The rocks are characterized by rather high contents of compatible elements (such as Ni and Cr), and incompatible elements such as (Ti, Zr, and P), and low contents of Y and Rb as compared with most basaltic rocks (Prinz 1967).

Variation diagrams of major and minor elements plotted against the MgO content are shown in Fig. 8. Deviations from several trends are exhibited by some of the samples and are mainly due to the effect of the above mentioned processes. Chemically, samples of Group 2 differ from those of Group 1 by their slight increase of SiO_2 (av. 43.90%) and alkalies (av. $Na_2O = 0.41\%$, $K_2O = 0.19\%$), but cannot be distinguished from those of Group 1 in MgO-oxides plots. The correlation data of Group 1 samples presented in Table 2 support the current mineralogy of the rocks, except for highly oxidized ones.

Minor Element Geochemistry

The behavior and trends of trace elements within the studied rocks can be demonstrated by plotting the ratio of magmatic incompatible high field-strength elements (i.e. Ti, P, Nb, and Zr) and the compatible elements (Ni, Cr, Zn, Sr) against incompatible ones that act as an index of igneous differentiation, for example Zr (Pearce and Cann 1973; Erlank and Kable 1976; Hanson 1978; Pearce and Norry 1979 and McClean and Kranidiotis 1987). Several plots of oxides (not shown) and trace elements were used in this study; those plotted against Zr are shown in Fig. 9. It can be seen from the plots that most major oxides and some of the minor elements (Sr, Cu) are the most mobile components during low-grade metamorphism, while Al_2O_3, Ti, Nb, Ni, Cr and Co are less mobile.

The high positive correlation coefficient for some incompatible elements pairs (for example, Zr-TiO_2, Al_2O_3-Zr, Al_2O_3-TiO_2, Zr-Nb, and Nb-TiO_2) reflect either a large addition of these elements to the system or their in situ residual concentration (McClean and Kranidiotis 1987). Clinopyroxene (now pumpellyite, chlorite, epidote, and sphene) can hold appreciable amounts of titanium, particularly in slow cooling lava. Arndt *et al.* (1977) found that Ti enters the pyroxene structure in large amounts at high crystal growth and low diffusion rates. The Ti/Zr-Zr plot and the high association of TiO_2 content with relatively low FM value (Fig. 10) might indicate a post-eruptive redistribution of Ti, rather than direct magmatic control. Phosphor-

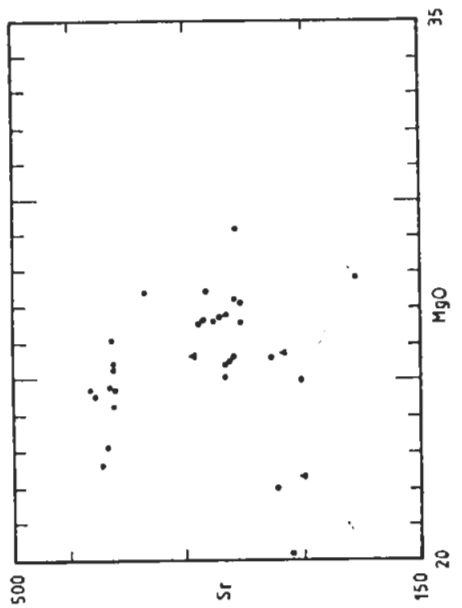

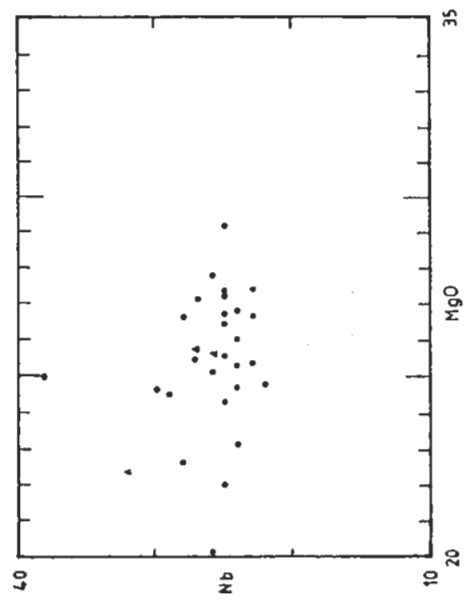

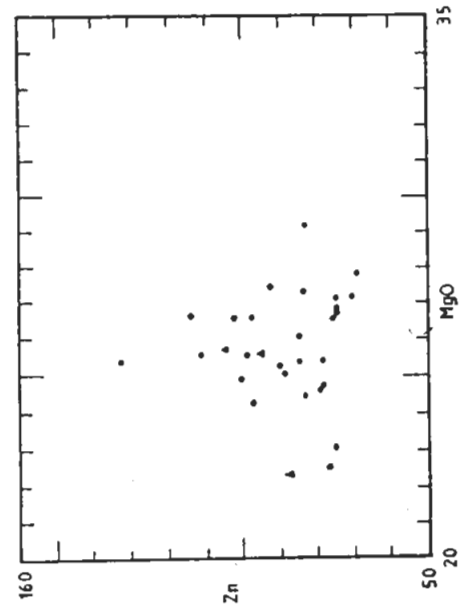

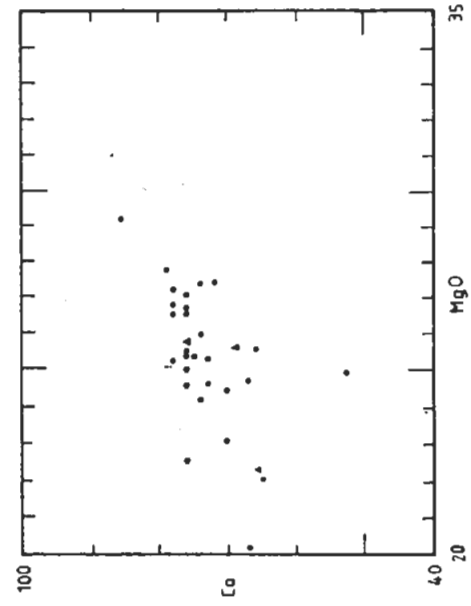

FIG. 8. Plots of major oxides (wt %) and minor elements (ppm) vs MgO content. Circles = Samples of Group 1; Triangle = Samples of Group 2.

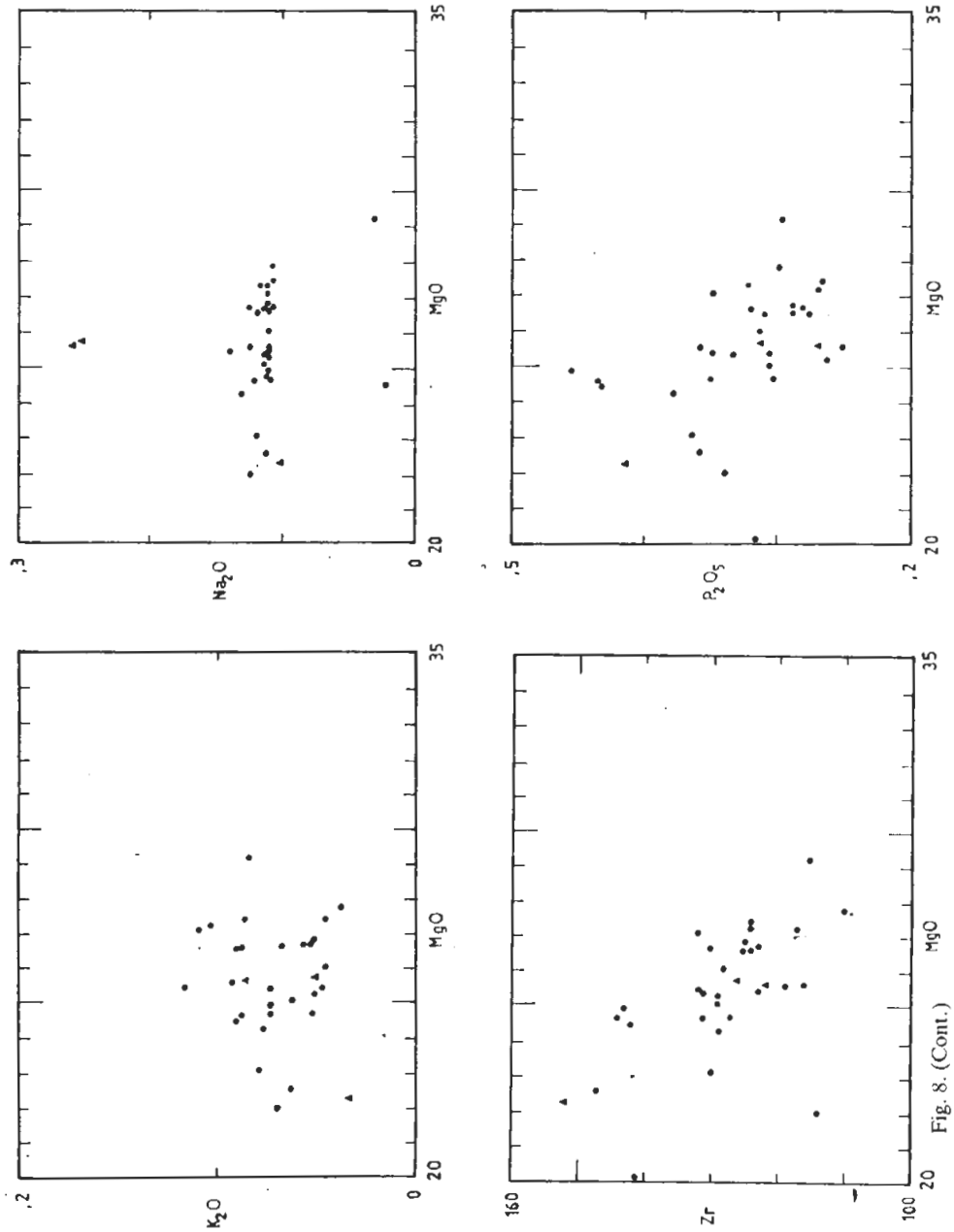

Fig. 8. (Cont.)

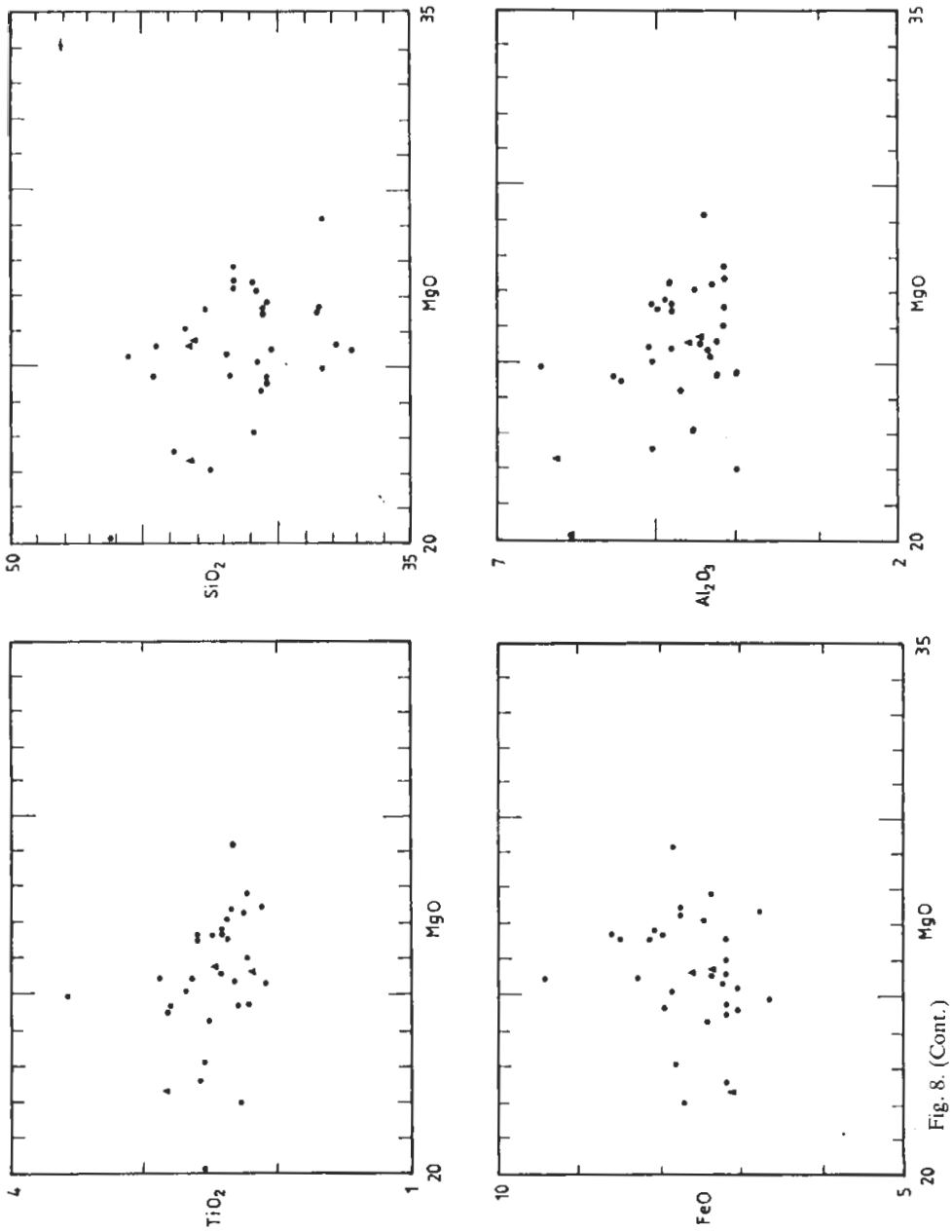
50
35
SiO_2
35
20
MgO
7
2
Al_2O_3
35
20
MgO
4
1
TiO_2
20
MgO
10
5
FeO
35
20
MgO

Fig. 8. (Cont.)

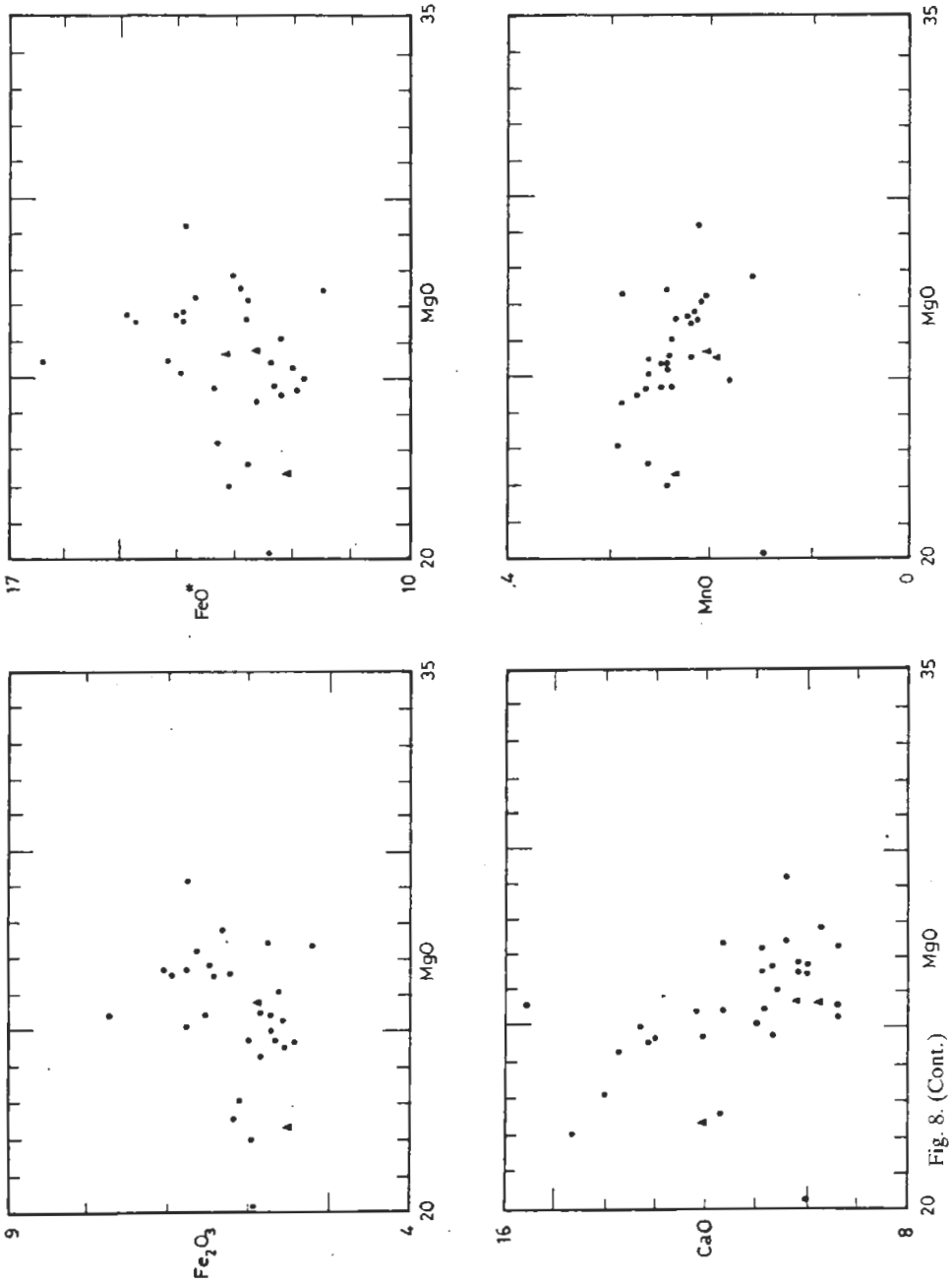

Fig. 8. (Cont.)

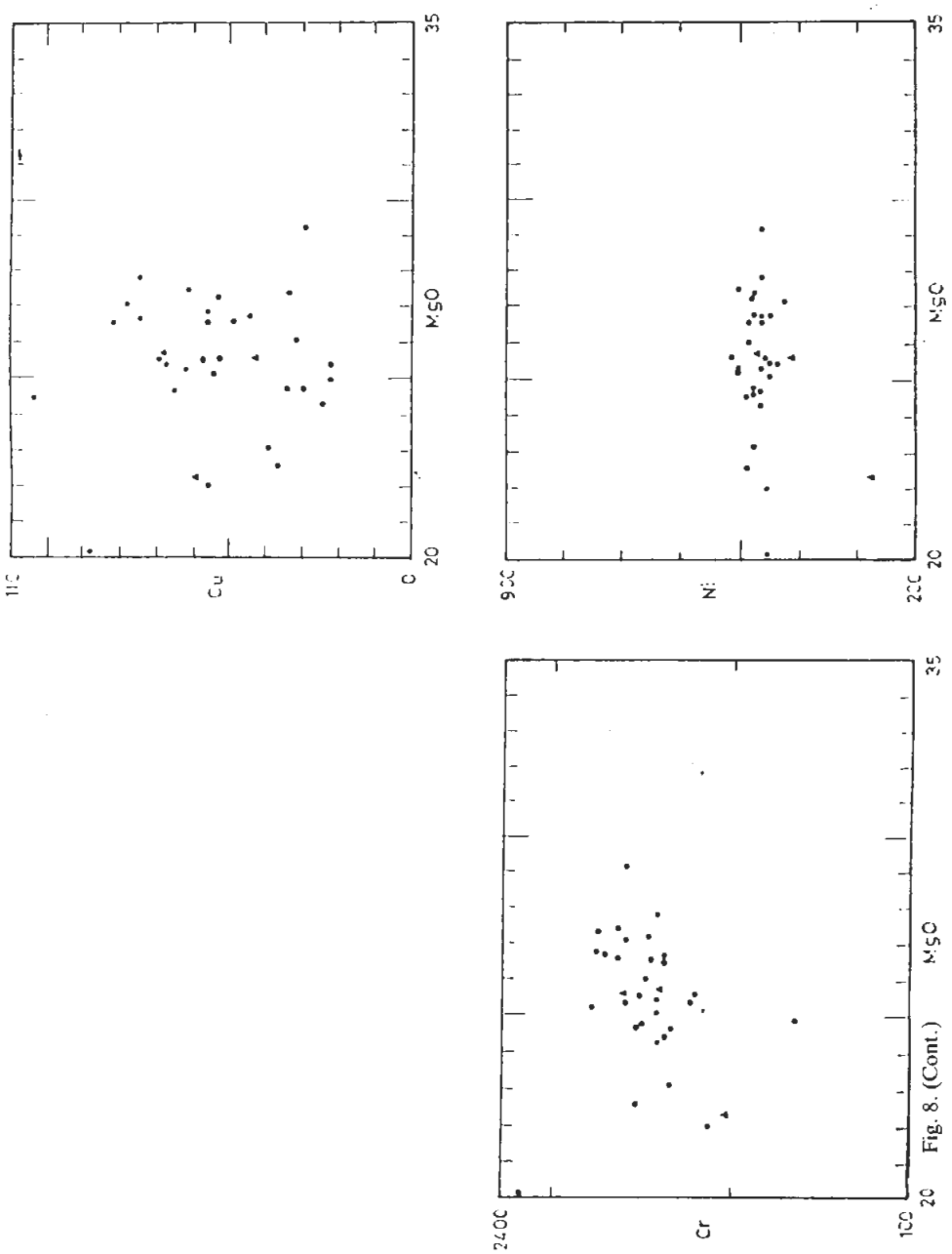

Fig. 8. (Cont.)

TABLE 2. Correlation matrix of major oxides and minor elements of 33 samples from Utma area, Y.R. (significance is 0.0001).

	SiO_2 (1)	TiO_2 (2)	Al_2O_3 (3)	Fe_2O_3 (4)	FeO (5)	MnO (6)	MgO (7)	CaO (8)	Na_2O (9)	K_2O (10)	P_2O_5 (11)	H_2O+ (12)	H_2O- (13)	Cu (14)	Ni (15)	Sr (16)	Zr (17)	Cr (18)	Co (19)	Zn (20)	Nb (21)
(1)					0.20	0.27	0.58	-0.21	0.23	-0.23		-0.26		-0.38	0.23	0.20		0.47	0.16	-0.20	-0.20
(2)			0.91			-0.20		0.28			0.71				-0.83			-0.54	-0.45	-0.20	-0.87
(3)							0.20	0.16			0.61	0.15			-0.64		0.66	-0.23	-0.25	-0.25	0.73
(4)					0.86	-0.48	0.50	-0.66			-0.49	-0.31					-0.49	0.26	0.54	-0.34	
(5)						-0.33	0.49	-0.74		-0.23	-0.62	-0.38	0.27	0.20	0.22	-033	-0.30	0.47	0.55	-0.34	-0.37
(6)							-0.23	0.29					0.33	-0.32	0.38	0.76	-0.45	0.36			-0.22
(7)								-0.50			-0.27	-0.31				-0.30	-0.30	0.52	0.44	-0.38	
(8)											0.73	0.41	-0.45	-0.22	-0.37	0.20	0.35	-0.50	-0.67	0.38	0.33
(9)														-0.24							
(10)											0.15	0.35		-0.20							0.23
(11)															-0.60	0.23	0.72	-0.53	-0.55		0.71
(12)													-0.46	0.26		-0.26	-0.20		-0.33		-0.20
(13)															0.30	-0.58	0.33	0.46	0.46	-0.33	-0.23
(14)															0.23	-0.29			0.20		
(15)																0.38	-0.30	0.73	0.67		0.79
(16)																	0.58	0.34			-0.24
(17)																		-0.20	-0.39		0.53
(18)																			0.71	-0.35	-0.72
(19)																				-0.39	-0.47
(20)																					

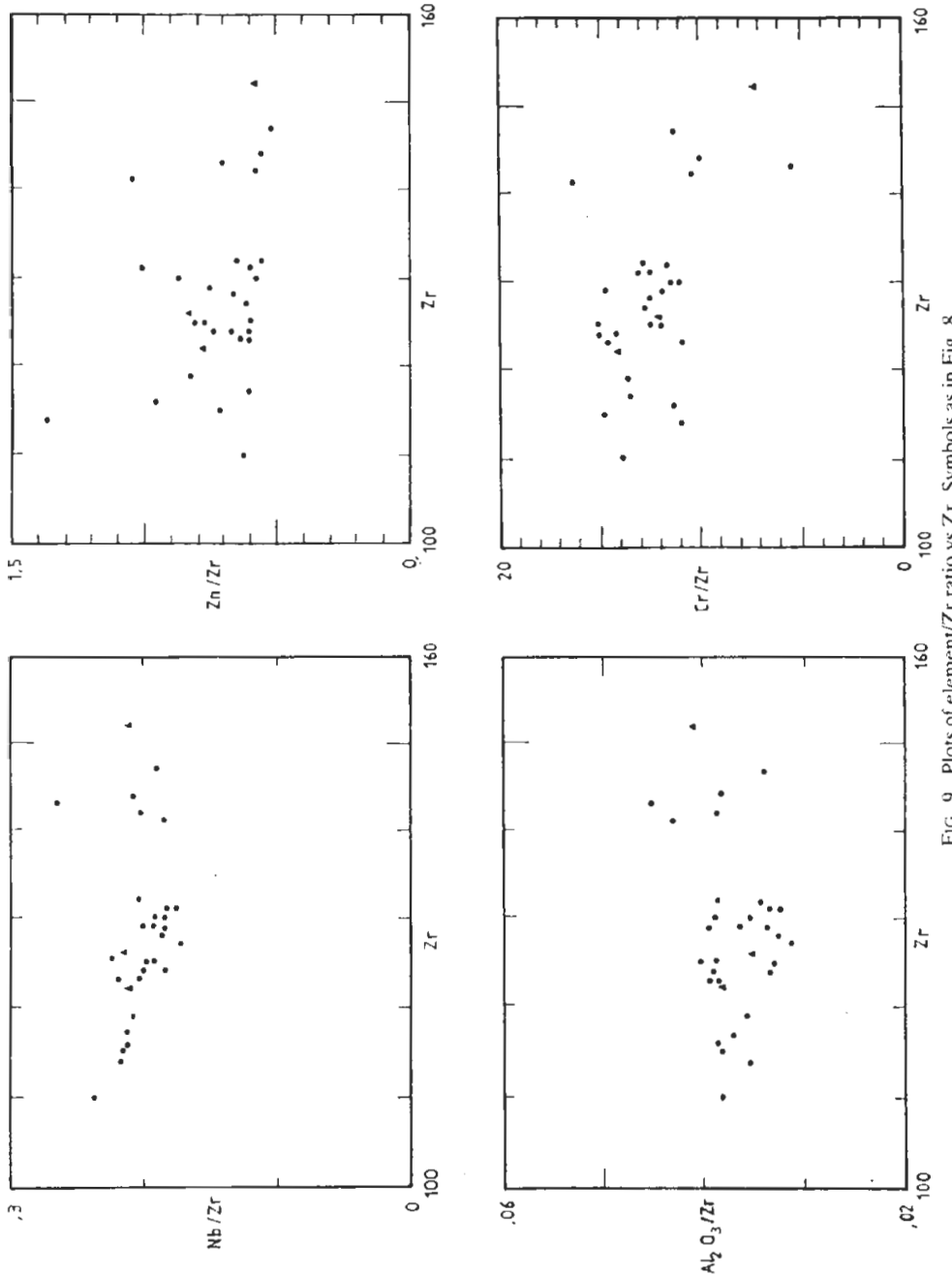

FIG. 9. Plots of element/Zr ratio vs Zr. Symbols as in Fig. 8.

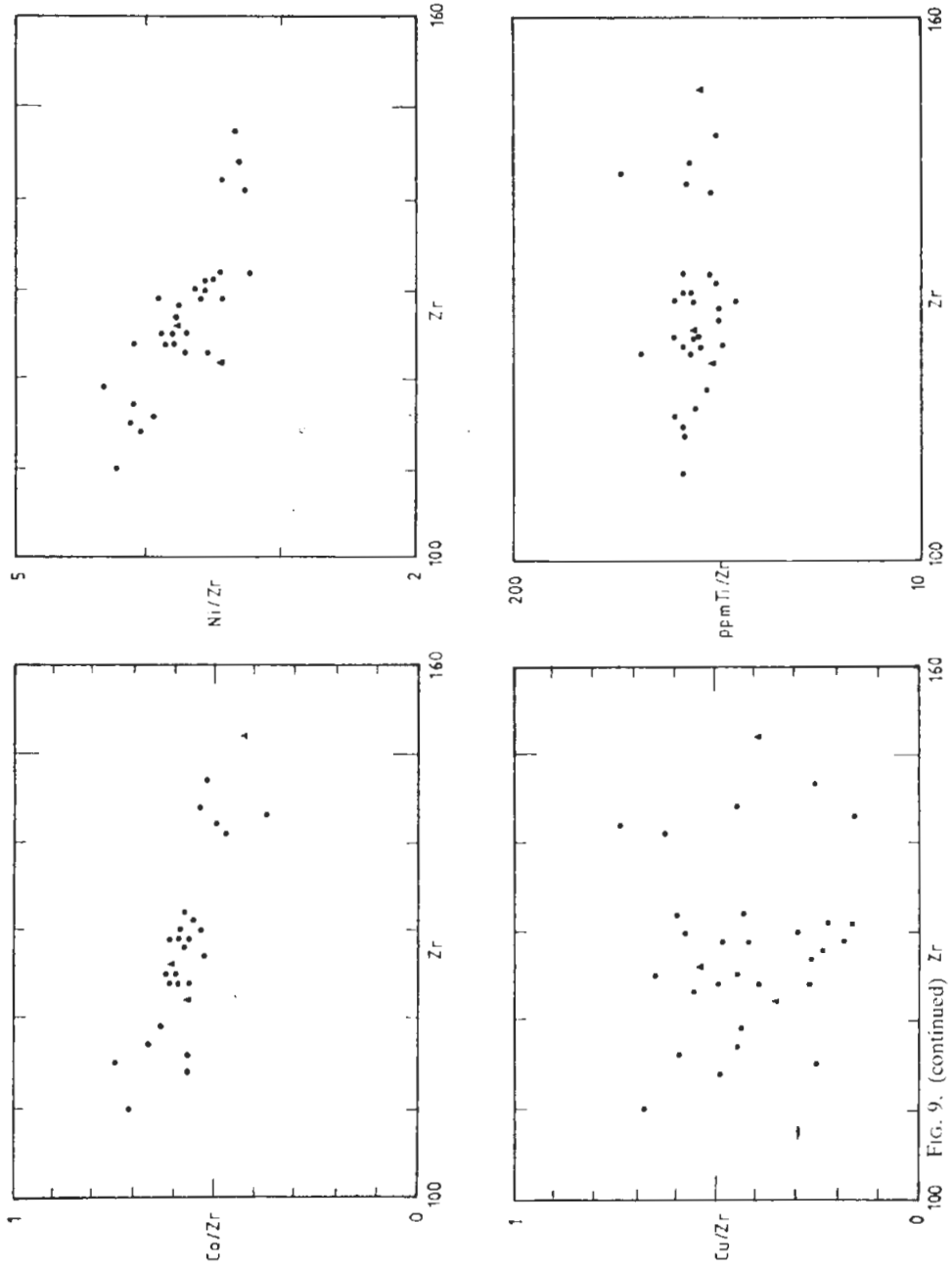

FIG. 9. (continued) Zr

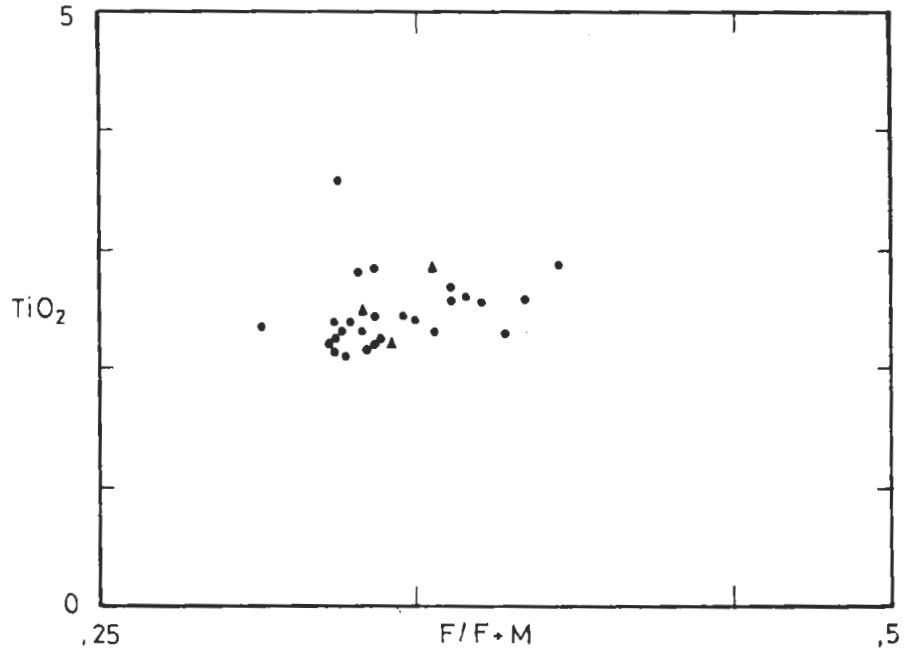

FIG. 10. Plot of TiO_2 (wt %) vs F/F+M [FeO/FeO+MgO] ratio. Symbols as in Fig. 8.

ous can be incorporated in the augite lattice. Its good correlation with the other incompatible elements and absence with K_2O might suggest a late stage precipitation of apatite. This is supported by the presence of small, prismatic apatite inclusion amongst the clinopyroxene crystals. Nickel content, on the other hand, for all samples of Group 1 and Group 2 is relatively similar, except for one sample (# 9) which shows a low value of 122 ppm. The Ni content is high (av = 460 ppm) compared to basaltic rocks but rather low compared to peridotite komatiitic liquid (av = 1200 ppm). Normally, Ni and TiO_2 contents of mafic lavas are both strongly affected by shallow-level magmatic differentiation (Wood 1978). In general, Ni is depleted and TiO_2 is enriched by the removal of mafic silicate, a process which also increases the FM ratio of the residual magma. Scatter but decrease of Ni with Zr reflects the effect of later low-grade metamorphism, when Ni was redistributed and reconcentrated in the amygdaloidal parts of the rocks. The Cr trend, in the MgO-Cr (Fig. 8) and the Cr-Zr (Fig. 9) plots suggest a magmatic differentiation of the Cr, where it has been extracted from the melt as olivines and clino-pyroxenes crystallize.

Metamorphic Differention and its Effect on Whole Rock Chemistry

Migration and behavior of major, minor, and trace chemical components during metamorphism of various rock types and ages have been described by Vallance (1965); Smith (1967); Jolly and Smith (1972); Condie (1976); Viljoen and Kable (1977); Jolly (1980); Smith *et al.* (1982); Fischer and Schmincke (1984) and Wood

and Graham (1986). The mineralogical assemblage of the studied rocks shows that deuteric alteration was overlapped and accompanied by late crystallization of pyroxene and operated under both low temperature and increasing H_2O partial pressure as the flows cooled. The degree of alteration is a function of the availability of water, permeability, and primary volcanic glass. Water was derived diagenetically from the serpentinization of olivine phenocrysts and chloritization of primary glass. With further cooling pyroxenes were altered into chlorite, pumpellyite, and sphene, with an intermediate amphibole (tremolite-actinolite) stage. Unwanted Ca^{++} ions went to form epidote which is embedded in the chlorite or filling amygdales. Hydration of glass and olivine led to the formation of chlorite, serpentine (antigorite), talc, and iron oxides. Calcium-rich plagioclase was altered to chlorite which leaches Al, while Si and Ca reacted to form amygdaloidal prehnite. Pumpellyitization of pyroxene and possibly plagioclase can cause release of Si to form amygdaloidal quartz. Iron (Fe^{+++}), partly went into magnetite, which was oxidized to hematite and might have partly been incorporated into pumpellyite (Surdam 1968). Hematite, is stable at high oxygen fugacity, so it must have developed as a result of near surface, exogenous oxidation (Lincoln 1981) or as a result of endogenous, syngenetic oxidation due to contamination of the parental magma with oxygen prior to eruption (Surdam 1968). Petrographical evidence suggests that hematite was formed as a result of deuteric alteration of cooling flows, following lava extrusion. The absence of hematite, but presence of some magnetite in pumpellyite, suggests that hematite was converted first, followed by magnetite during pumpellyite producing reactions. This reaction is an important factor in copper distribution and precipitation, as will be seen later. Further, and with the progress of alteration, particularly clinopyroxenes (augite and possibly titanoaugite) and adjacent iron-oxides sphene and hematite, along with finely disseminated native copper, formed within the host silicate minerals, where the latter appears to have been exsolved as the iron oxidized.

The movement of the major components and the main alteration products that were formed during deuteric alteration and low-grade metamorphism are summarized in Fig. 11.

Discussion

The composition of the lower (Groups 1 and 2) sequence of mafic volcanic rocks at Utma is peculiar and closely resembles that of the basaltic, low Al-komatiites of the Barberton Mountain Land (Viljoen and Viljoen 1969, 1971); Brooks and Hart's (1974) adopted class of high magnesian and calcium, and low alkalies and alumina contents; Naldrett and Gabri's (1976) class of effusive rocks; and the komatiitic flows described by Arndt (1986). The petrographical and chemical evidence from the present study suggests that this sequence represents non-cumulate pyroxene rocks (komatiitic in nature) of effusive origin, that were emplaced at shallow depths and crystallized under low fO_2 conditions. These rocks differ from the above mentioned true komatiites in their high $FeO/(FeO+MgO)$, CaO/Al_2O_3, and TiO_2, and low Al_2O_3 contents. The high TiO_2 content of these rocks is similar to that of the Ar-

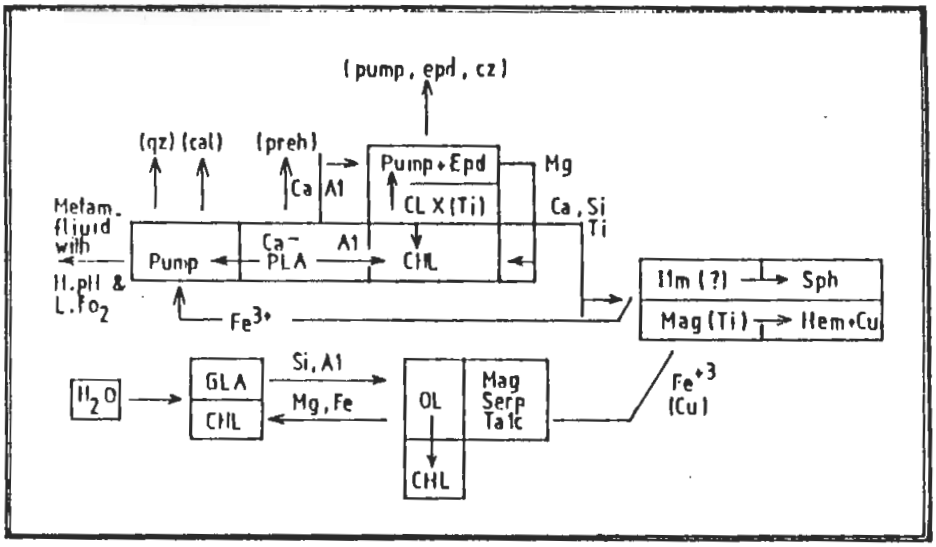

FIG. 11. Sketch diagram showing possible element mobilization and formation of secondary products during alteration and low-grade metamorphism. Pump = pumpellyite, epd = epidote, cal = calcite, preh = prehnite, chl = chlorite, gla = glass, ol = olivine, mag = magnetite, serp = serpentine, ilm = ilmenite, sph = sphene.

chaean tholeiites described by Williams (1972). The Al_2O_3/TiO_2 ratio of the Utma rocks is lower than that of the Barberton rocks, which implies either retention of Al_2O_3 in the residue or loss of Al_2O_3 before melt extraction (Smith and Erlank 1982).

CIPW norms (Table 1) show that nearly all samples of Groups 1 and 2 contain significant amounts of normative olivine, diopside, and anorthite. Twelve samples of these (including the four samples of Group 2) contain normative hypersthene. Minor constituents are normative magnetite, ilmenite, and apatite. The apparent norm values have been modified by low-grade metamorphism. For instance, the high Fe_2O_3/FeO ratio of the oxidized rocks leads to large quantities of magnetite in the norms, which enhances the formation of hypersthene. Further, the high TiO_2 content causes the appearance of ilmenite in the norm calculations. It can be concluded from the norm analyses that the rocks of Group 1 and Group 2 are undersaturated olivine tholeiites of Mg-rich lava and undersaturated hypersthene Mg-rich lava, respectively.

The absence of direct magmatic precipitation of orthopyroxene, the scattered but decreasing content of Ni and Cr with increasing Zr (Hart and Davis 1978), and the enrichment of TiO_2 with increasing Zr (Irvine and Baragar 1971) all suggest a tholeiitic magma of olivine, clinopyroxene, and plagioclase fractionation (Jolly 1975). Equant olivine crystals are thought to have formed under a slow rate of cooling or to represent mantle xenoliths of primary magma (Arndt *et al.* 1977).

Inspite of the low-grade metamorphism that affected the studied rocks, an attempt will be made to look at the petrogenesis and possible type of these rocks (tholeiitic vs.

komatiitic lavas), in the light of a number of geochemical criteria that have been used to discriminate the two types (Nesbitt and Purvis 1979; Distler and Genkin 1980; Rajamani *et al.* 1985). The analyzed samples can be compared with representative samples of komatiitic rocks from the Barberton Mountain Land, S. Africa (Viljoen and Viljoen 1971); komatiitic flows from Munro Township, Canada (Arndt *et al.* 1977); metavolcanites from Noril'sh and Pechenga provinces, USSR (Distler and Genkin 1980); Kolar amphibolites, South India (Rajamani *et al.* 1985); and with the komatiite average composition (Viljoen and viljoen 1969) (see Table 1 and Fig. 12).

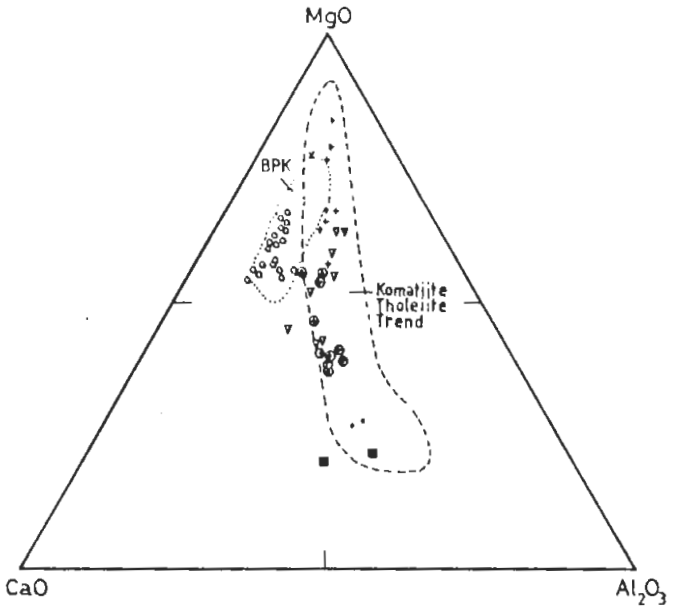

FIG. 12. CaO-MgO-Al_2O_3 ternary diagram. Symbols as follows: (o) = Utma Group 1 & Group 2 rocks; (+) = Komatiites, Munro Township, Canada (Arndt *et al.* 1977); (▽) = Picritic metavolcanics (komatiites) and picritic basalts, Noril'sh and Pechenga provinces, USSR (Distler and Genkin 1980); (⊕,●) = Kolar komatiites and Kolar tholeiites, S. India (Rajamani *et al.* 1985); (x) = Average composition of komatiites (Viljoen and Viljoen 1969); (■) = Basalt of Tertiary Yemen Volcanics (this study). BPK (Barberton komatiitic rocks) and Komatiite-tholeiite trend field are taken from Rajamani *et al.* 1985.

The plots show that the analyzed rocks cluster within the Barberton Mountain Land field. The slight deviation of the trend towards the CaO-MgO side is due to the subsequent low-grade metamorphism (serpentinization of olivine and chloritization of pyroxenes). Furthermore, the plot of FM vs. Al_2O_3 (Fig. 13) shows that the studied rocks, along with the low Al_2O_3 komatiitic rocks of the Barberton Mountain Land (Viljoen and Viljoen 1969) lie in the field of tholeiites. Two samples fall in the cumulate komatiite field and one sample falls in the komatiitic flow portion of the plot (possibly due to alteration). In conclusion, we can say that samples of Group 1 and Group 2 represent a noncumulate pyroxenite rocks of extrusive origin that were emplaced and contaminated at shallow levels.

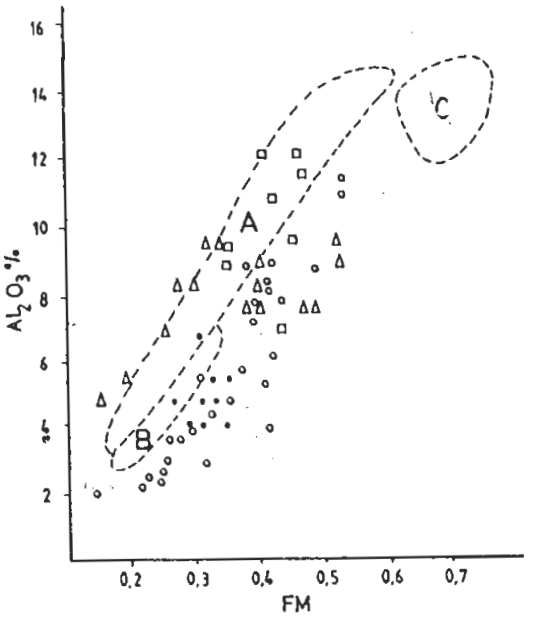

FIG. 13. Plot of Al_2O_3 vs FM. Symbols as follows: (•) = Utma Group 1 & Group 2 rocks; (o) = Barberton komatiitic rocks, S. Africa; (□) = Picritic metavolcanics (komatiites) and picritic, Noril'sh and Pechenga provinces, USSR; (△) = Kolar komatiites, S. India. Fields A, B, and C represent komatiitic flows, cumulate rocks, and tholeiitic basalts, respectively, Munro Township, Canada. [All data are taken from references listed in caption to Fig. 12].

In general, the structural environment of the Tertiary Yemen volcanics in the central highlands favors the presence of a shallow level magma chamber as concluded by Chiesa *et al.* (1983) in the Dhamar area.

The origin of these effusive rocks and whether they are genetically related to the overlying tholeiitic rock series or represent a different magma series, needs a further investigation.

Copper Mineralization

The nature and origin of native copper in rocks of similar composition has been discussed by many authors (for example, White 1968, 1971; Jolly 1974; Lincoln 1981; Eilenberg and Carr 1981). Copper analyses of samples from the lower parts of the Utma sequence are given in Table 1. The copper content varies from 29 to 104 ppm (sample # 2). This is comparable to estimates of copper contents in various similar rocks which are 28 to 103 ppm (Zlobin *et al.* 1973). Study of polished sections shows that native copper, with other secondary minerals, is distributed as fine grains (locally < 0.1 mm in diameter) in the amygdales and within the silicate minerals, and as veinlets associated with hematite in pseudomorphs after clinopyroxenes and possibly

olivine. With increasing of alteration, such as is found along fractures, native copper is present as flakes large enough to be visible in hand specimens and sufficient to be economically important (Fig. 14).

FIG. 14. Two photographs of polished section showing disseminated and veinlets of native copper (cu) in the amygdaloidal portion of the rock, sample # 14, (×100).

Careful examination of some polished sections indicates that the pattern of native copper distribution is affiliated to the pattern of oxidation of the iron-bearing minerals. Advanced oxidation of augite (titanaugite), olivine, and primary iron oxides leads to the formation of symplectic hematite with magnetite texture and a hematite diffusion rim, which increases towards the grain boundary. This phenomenon has been observed in the native copper of the Keweenawan district (Livnat 1983). Release of copper from the margins of the silicate minerals seems to be synchronous with its metamorphic alteration, or more closely with pumpellyitization processes, in which the copper is lost from the host silicate minerals and reprecipitated epigenetically in fractures and amygdales.

Source and Origin of Copper

Clinopyroxene (augite) and iron oxides are the minerals that most strongly affect the behavior of copper in mafic magma differentiation (Livnat 1983). In this study, two samples that contain many phenocrysts and lack amygdales were crushed and separated by bromoform liquid. Copper analysis of the separated silicate and iron fractions revealed that the former contains higher copper concentration (60 ppm) compared to the later (30 ppm). In part, this is due to the unlikely substitution of Cu^{++} in the spinel structure of the magnetite (Burns and Fyfe 1967). It is evident that

the silicate minerals, especially augite, are the main source of syngenetic copper, which have been reworked by later metamorphic processes and redeposited in amygdales and fracture zones. So the deposition of copper within the Utma lower rock sequence is probably a combination of both syngenetic and epigenetic processes.

The importance of the chemistry of the metamorphic solutions on the distribution and precipitation of native copper was discussed by Lincoln (1981) and Livnat (1983). Generally, pumpellyitization of primary mineral phases can cause either consumption of H^+ ions (*i.e.* raise the pH), or lower the fO_2 of the metamorphic fluids. Both conditions favour the precipitation of native copper. Furthermore, the absence of hematite and presence of magnetite within the pumpellyite phase suggests that low fO_2 metamorphic fluids entered the mineral assemblage in the rock causing the precipitation of native copper.

The absence of copper sulphides in the study area might be due to the continuous degassing of volatiles (SO_2) during and after lava eruption in an oxidizing environment, which produces S-deficient lava flows.

Relative shallow depth of burial, the abundance of joints, fractures, and the presence of relic phenocrysts support the possibility that the metamorphic fluid pressure was less than the total pressure during metamorphism.

Conclusion

Petrographic study of representative samples from the lower part of the Tertiary Utma volcanics shows that they represent non-cumulate pyroxenite rocks that were emplaced at shallow depths. The rocks are composed of phenocrysts of relict, skeletal, and rarely zoned clinopyroxene and skeletal olivine embedded in fine-grained clinopyroxene, ca-plagioclase, magnetite, glass, and other low-temperature Al-silicate minerals. Porphyritic, intergranular, and cluster textures are predominant. Geochemical analyses and norm calculations show that the rocks are under-saturated tholeiitic Mg-rich lavas. Geochemical comparison of the analyzed samples with others from various parts of the world show that the Utma lower sequence lies within the low Al_2O_3 komatiitic field of the Barberton Mountain Land and is characterized by high TiO_2 and F/(F+M) values and possibly is not komatiite.

Ore microscopy reveals the presence of very fine-grained disseminated, veinlets, and amygdales-filled with native copper. This study shows that the silicate minerals are the source of syngenetic copper; copper was leached and reconcentrated epigentically in amygdales and fractures, along with hematite. Pumpellyitization of primary minerals produced metamorphic fluids with favorable geochemical conditions for the precipitation of native copper.

Acknowledgement

We want to express our thanks to Sana'a University for providing us with the transportation to the field, and to the people at the Central Research Lab., Faculty of Sci-

ence for giving us access to the XRF unit. Much gratitude is extended to Prof. M. El Aissawi for reading the first draft of this manuscript. Special thanks to Mr. Abdul-Rakib Terkstany for carrying out the XRD analyses at the Jeddah-USGS Lab. Also we would like to thank Mrs. Baha Mahmood and Mr. A. Eisawi for their nice drafting.

References

Almond, D.C. (1986) The relation of Mesozoic-Cenozoic volcanism to tectonism in the Afro-Arabian dome, *J. Volcan. Geoth. Res.* **28:** 225-246.

Arndt, N.T. (1986) Differentiation of komatiite flows, *J. Petrol.* **27:** 279-301.

Arndt, N.T., Naldrett, A.J. and **Pyke, R.** (1977) Komatiitic and iron-rich tholeiitic lavas of Munro Township, Northern Ontario, *J. Petrol.* **18:** 319-369.

Augustithis, S.S. (1978) *Atlas of textural patterns of basalts and their genetic significance*, Amsterdam, Elsevier Sci. Co., 323p.

Brooks, C. and **Hart, S.R.** (1974) On the significance of komatiite, *Geology* **2:** 107-110.

Burns, R.G. and **Fyfe, W.S.** (1967) Crystal-field theory and the geochemistry of transition elements, *In:* **Abelson, P.H. (ed.),** *Researches in Geochemistry* **2:** 1-19.

Camp, V.E. and **Roobol, M.J.** (1989) The Arabian continental alkali basalt province: Part I. Evolution of Harrat Rahat, Kingdom of Saudi Arabia, *Geol. Soc. Am. Bull.* **101:** 71-95.

Capaldi, G., Chiesa, S., Manetti, P., Orsi, G. and **Poli, G.** (1987a) Tertiary anorogenic granites of the Western Border of the Yemen Plateau, *Lithos* **11:** 433-444.

Capaldi, G., Chiesa, S., Civetta, L., La Volpe, L., Manetti, P., Orsi, G. and **Piccardo G.B.** (1987b) Magmatic and tectonic activities in North Yemen during Tertiary and Quaternary times, *Mem. Soc. Geol., Ital.* **XXIX:** 154-165.

Capaldi, G., Chiesa, S., Conticelli, S., and **Manetti, P.** (1987c) Jabal An Nar: an Upper Miocene volcanic centre near Al Mukha, Yemen Arab Republic, *J. Volcanol. Geotherm. Res.* **31:** 345-351.

Carr, M.J. (1985) IGPET: *Basic tools for igneous petrology*, New Brunswick, Rutgers Univ.

Chiesa, S., Bergano, L., La Volpe, L., Lirer, B.L., Napoli, and **Orsi, G.** (1983) Geology and structural outline of Yemen Plateau, YAR, *N. Jb. Geol. Paleontol. Mh.* **11:** 641-656.

Civetta, L., La Volpe, L. and **Lirer, L.** (1978) K-Ar ages of the Yemen Plateau, *J. Volcanol. Geoth. Res.* **4:** 307-314.

Condie, K.C. (1976) Trace element models for the origin of Archean volcanic rocks, *In:* **Windley, B.F. (ed.)** *Early History of the Earth*, London, John Wiley and Sons, 419-424.

Distler, V.V. and **Genkin, A.D.** (1980) Deposits of sulfide copper-nickel ores of the USSR and their connection with cratonal volcanism, *Proceedings of the Fifth Quadren nial IAGOD Symp., Germany*, pp. 275-295.

Eilenberg, S. and **Carr, M.J.** (1981) Copper contents of lavas from active vocanoes in El Salvador and adjacent regions in Central America, *Econ. Geol.* **76:** 2246-2248.

Erlank, A.J. and **Kable, E.D.** (1976) The significance of incompatible elements in Mid-Atlantic Ridge basalts from 45 N with particular reference to Zr/Nb, *Contrib. Mineral. Petrol.* **54:** 281-291.

Fischer, R.V. and **Schmincke, H.U.** (1984) *Pyroclastic rocks*, New York, Springer-Verlag, 472p.

Gass, I.G. (1970) The evolution and volcanism in the junction area of the Red Sea, Gulf of Aden, and Ethiopian rifts, *Phill. Trans. Roy. Soc. London*, **A.267:** 369-381.

Guekens, F. (1966) Geology of Arabian Peninsula, a review of the geology of Yemen (translated from French by S.D. Bowers), *U.S. Geol. Surv., Prof. Paper 560B:* B1-B23.

Gladney, E.S. and **Goode, W.E.** (1981) Elemental concentrations in eight new United States Geological Survey rock standards: A review, *Geostand. Newsl.* **5:** 31-6.

Grolier, M.J. and **Overstreet, W.C.** (1978) Geological map of the Y.A.R., *U.S. Geol. Surv., Misc. Invest ig. Series, Map* **I-1143-B,** 1:500,000 scale.

Hanson, G.N. (1978) The application of trace elements to the petrogenesis of igneous rocks of granitic composition, *Earth Planet. Sci. Lett.* **38:** 26-43.

Hart, S.R. and **Davis, K.E.** (1978) Nickel partitioning between olivine and silicate melt, *Earth Planet. Sci. Lett.* **40:** 203-219.

Heychendorf, K. and **Jung, D.** (1989) Tertiary Trap volcanism of the Yemen Arab Republic, *Paper presented at the XIV General Assembly of the European Geophy. Soc.*, March 15, 1989, 16p.

Hintze, J.L. (1986) *NCSS-Number Cruncher Statistical System*, v. 4.21, Kaysville, Utah.

Huchon, P., Jestin, F., Cantagrel, J.M., Gaulier, J.M. and **Al-Khirbash, S.A.** (1990) Extensional deformations in the Oligo-Miocene Trapps of Yemen, *Abstract at the European Union of Geologic Meeting*, March, 1991.

Hutchison, C.S. (1974) *Laboratory handbook of petrographic techniques*, New York, John Wiley and Sons, Inc., 527p.

Irvine, T.N. and **Baragar, W.A.** (1971) A guide to the chemical classification of some common volcanic rocks, *Cand. J. Earth Sci.* **8:** 523-548.

Johnson, W.M. and **Maxwell, J.A.** (1981) Rock and mineral analysis, *In:* **Elving, P.J.** and **Winefordner, J.D. (eds.)** *A series of monographs on analytical chemistry and its applications* **27:** New York, John Wiley and Sons, pp. 121-182.

Jolly, W.T. (1974) Behavior of Cu, Zn, and Ni during prehnite-pumpellyite rank metamorphism of the Keweenawan basalts, North Michigan, *Econ. Geol.* **69:** 1118-1125.

Jolly, W.T. (1975) Subdivision of the Archean lavas of the Abitibi area, Canada, from Fe-Mg-Ni-Cr relations, *Earth Planet. Sci. Lett.* **27:** 200-210.

Jolly, W.T. (1980) Development and degradation of Archean lava, Abitibi area, Canada, in light of major element geochemistry, *J. Petrol.* **21:** 323-363.

Jolly, W.T. and **Smith, R.E.** (1972) Degradation and metamorphic differentiation of the Keweenawan tholeiitic lavas of Northern Michigan, USA, *J. Petrol.* **13:** 273-309.

Kruck, W. (1983) *Geological map of the Yemen Arab Republic*, sect Sana's 1:250,000-Hannover (Fed. Inst. Geosci. Nat. Res.).

Lincoln, T.N. (1981) The redistribution of copper during low-grade metamorphism of the Karmutsen volcanics, Vancouver Islands, British Columbia, *Econ. Geol.* **76:** 2147-2161.

Livnat, A. (1983) *Metamorphism and copper mineralization of the Portage Lake lava series, North Michigan*, Ph.D. Thesis, Univ. of Michigan, 262 p. (Unpublished).

McClean, W.H. and **Kranidiotis, P.** (1987) Immobile elements as monitors of mass transfer in hydrothermal alteration: Phelps Dodge massive sulfide deposit, Matagami, Quebec, *Econ. Geol.* **82:** 951-962.

Menzies, M., Bosence, D., El-Nakhal, H., Al-Khirbash, S., Al'Kadasi, M. and **Al-Subbary, A.** (1990) Lithospheric extension and the opening of the Red Sea: *sediment-basalt relationships in Yemen, Terra Nova* **2:** 340-350.

Naldrett, A.J. and **Cabri, L.J.** (1976) Ultramafic and related mafic rocks: Their classification and genesis with special reference to the concentration of neckel sulfides and platinum elements, *Econ. Geol.* **71:** 1131-1158.

Nesbitt, R.W. and **Purvis, A.C.** (1979) Komatiites: Geochemistry and genesis, *Canad. Mineralogist* **17:** 165-186.

Overstreet, W.C., Kiilsgaard, T.H., Grolier, M.J., Schmidt, D.L., Domenico, J.A., Donato, M.M., Botinelly, T. and **Harms, T.F.** (1985) Contributions to the geochemistry, economic geology, and geochronology of the Yemen Arab Republic, *U.S. Geol. Surv., Proj. Rep.* **(IR) YE-17:** 152p.

Prinz, M. (1967) Geochemistry of basaltic rocks: Trace elements, *In:* **Basalts, V.I., Hess, H.H.** and **Poldervaart, A. (eds.)** *Interscience*, New York, John Wiley, Inc., pp. 271-323.

Pearce, J.A. and **Cann, J.R.** (1973) Tectonic setting of basic volcanic rocks determined using trace element analysis, *Earth Planet. Sci. Lett.* **19:** 290-300.

Pearce, J.A. and **Norry, M.J.** (1979) Petrogenetic implications of Ti, Zr, Y, and Nb variations in volcanic rocks, *Contrib. Mineral. Petrol.* **69:** 33-47.

Rajamani, V., Shivkumar, K., Hanson, G.N. and **Shirey, S.B.** (1985) Geochemistry and petrogenesis of amphibolites, Kolar schist belt, South India, Evidence for komatiitic magma derived by low percentages of melting of the mantle, *J. Petrol.* **26:** 92-123.

Smith, N.H. and **Erlank, A.J.** (1982) Geochemistry and petrogenesis of komatiites from the Barberton greenstone belt, South Africa, *In:* **Arndt, N.T.** and **Nisbet, E.G. (eds.)** *Komatiites*, London, Allen and Urwin, 347-397.

Smith, R.E. (1967) Redistribution of major elements in the alteration of some basic lavas during burial metamorphism, *J. Petrol.* **9:** 191-219.

Smith, R.E., Perdrix, J.L. and **Parks, T.C.** (1981) Burial metamorphism in the Hamersley Basin, Western Australia, *J. Petrol.* **23:** 75-102.

Surdam, R.C. (1968) Origin of native copper and hematite in the Karmutsen group, Butte Lake area, Vancouver Island, British Columbia, *Econ. Geol.* **63:** 961-966.

Vallance, T.G. (1965) On the chemistry of pillow lavas and the origin of spillites, *Mineral Mag.* **34:** 471-481.

Viljoen, M.J. and **Kable, E.D.** (1977) Effects of alteration on element distribution in Archean tholeiites from Barberton greenstone belt, South Africa, *Contr. Mineral. Petrol.* **64:** 75-90.

Viljoen, M.J. and **Viljoen, R.P.** (1969) The geology and geochemistry of the lower ultramafic unit of the Onverwacht Group and a proposed new class of igneous rock, *Upper Mantle Proj. Spec. Publs. Geol. Soc. S. Afr.* **2:** 221-244.

Viljoen, R.P. and **Viljoen, M.J.** (1971) The geological and geochemical evolution of the Onverwacht volcanic Group of the Barberton Mountain Land, South Africa, *Geol. Soc. Aust. Spec. Bull.*, No. **3.**

White, W.S. (1968) The native copper deposits of North Michigan, *In:* **Ridge, J.D. (ed.)** *Ore Deposits of the United States, 1933-1967. Am. Instit. Min.*, Metallurg. Petroleum Engineers, Inc., pp. 303-325.

White, W.S. (1971) A paleohydrologic model for mineralization of the White Pine copper deposit, North Michigan, *Econ. Geol.* **66:** 1-13.

Williams, D.A. (1972) Archean ultramafic, mafic, and associated rocks, Mt. Monger, Western Australia, *J. Geol. Soc. Aust.* **19:** 163-188.

Wood, B.J. and **Graham, C.M.** (1986) Infiltration of aqueous fluid and high fluid: rock ratios during greenschist facies metamorphism: A discussion, *J. Petrol.* **27:** 751-761.

Wood, D.A. (1978) Major and trace element variation in the Tertiary lavas of Eastern Iceland and their significance with respect to the Iceland geochemical anomaly, *J. Petrol.* **19:** 393-436.

Zlobin, B.I., Kravchenko, S.M. and **Laktionova, N.V.** (1973) Distribution of copper in the extrusive basaltic series of different alkalinity, *Geochem. Int.* **10:** 270-276.

بترولوجيـــة وجيوكيميائيـــة النحـاس لصخـــور الجـزء الأسفـــل من بركـانيـــات اليمـــن منطقـــة عتمـــة - الجمهوريـــة اليمنيـــة

صلاح ع . الخرباش و طارق هـ . الحبشي

قسم الجيولوجيا ، كلية العلوم ، جامعة صنعاء ، صنعـــاء ، الجمهوريـة اليمنية

المستخلص . تضمنت هذه الدراسة فحص مجهري وتحليل كيميائي لبعض عينات الجزء الأسفل من صخور بركانيات اليمن المنكشفة في منطقة عتمة والتي ترجع للحقب الثلاثي . من خلال الدراسات المجهرية وجد أن هذا الجزء يتكون من صخور غير تراكمية تدفقية الأصل ذو تركيب مافي ضحل المنشأ . تتركب هذه الصخور من معادن الكلينوبيروكسين (الأوجيت والتيتانوأوجيت ؟) ، الأوليفين ، والبلاجيوكلز الكلسي والموجودة على هيئة نسيج بورفري ، بين حبيبي ، وأحيانًا نسيج اسبينفيكسي .

أما معطيات التحاليل الكيميائية فقد دلت على أن هذه الصخور تكونت من صهير ثولييتي تحت مشبع وتحتوي على نسب عالية من أكاسيد المغنسيوم ، الحديد ، والتيتانيوم ، وعناصر النيكل والكروم ، ونسب قليلة من أكاسيد السيليكا ، والألمونيوم ، والأكاسيد القلوية .

تعرضت هذه الصخور محليًا إلى سحنة متحولة منخفضة الحرارة مكونة معادن البمبيلايت ، الكلوريت ، الإبيدوت ، الأسفين ، وأكاسيد الحديد .

من خلال دراسة العلاقات الكيمياوية $CaO-MgO-Al_2O_3$ و Al_2O_3 مع FM لهذه الصخور ومقارنتها بصخور مماثلة من مناطق أخرى من العالم وجد أنها تشبه الصخور منخفضة عنصر الألومنيوم الموجودة في منطقة الباربرتون بجنوب أفريقيا (Viljoen and Viljoen, 1969) ، ولكنها ليست كومتايتة الأصل .

دلت دراسة المقاطع المصقولة على وجود ترسبات النحاس الخالص المترسب على هيئة حبيبات متناثرة وعروق صغيرة . أما نتائج النحاس لعينات مفصولة فقد دلت بأن المعادن السيلكاتية هي المصدر الأساسي للنحاس والذي بدورة رُشح أثناء عملية التحول واعيد ترسيبة بشكل واضح في الفراغات اللوزية وعلى سطوح المكاسر والفواصل .

المحاليل المتحولة الناتجة من عمليات تكون البمبيلايت مُيزت بخصائص كيميائية ملائمة لترسيب النحاس الخالص في صخور المنطقة .